Demarcation method of safety separations for sUAV based on collision risk estimation

基于碰撞风险估计的小型无人机安全隔离划分方法

Gang Zhong [a,*] , Sen Du [a] , Honghai Zhang [a] , Jiangying Zhou [a] , Hao Liu [b]
钟刚 [a,*] ， 杜森 [a] ， 张洪海 [a] ， 周江英 [a] ， 刘浩 [b]
[a] College of Civil Aviation, Nanjing University of Aeronautics and Astronautics, Nanjing, China
[a] 南京航空航天大学民航学院，南京，中国
[b] College of Science, Nanjing University of Aeronautics and Astronautics, Nanjing, China
[b] 南京航空航天大学理学院，南京，中国

A R T I C L E I N F O

文章信息

Keywords:
关键词:
UAV separation criteria
无人机隔离标准
Collision risk model
碰撞风险模型
Equivalent level of safety
安全等效等级
Sensitivity analysis
敏感性分析
Low-altitude airspace design
低压空域设计

A B S T R A C T

摘要

Maintaining safe separations is essential to achieve reliable operations for unmanned aerial vehicles (UAV). Given the escalating severity of collision risks associated with UAVs, separation criteria have emerged as foundational to both airspace design and collision avoidance strategies. However, without adequate consideration of the characteristics of small-UAV (sUAV) encounters and airspace structure, most of the existing models focus on assessing uniform separation volume with manned aircraft. This paper proposes a demarcation method of safety separation for sUAVs based on collision risk estimation. Firstly, five collision zones are developed for collision determination by considering the shape characteristics. Then, the collision risk model is established from the 3-D probability density function (PDF) with the supremum of total system error (TSE). Finally, the minimum safe separations for different encountering scenarios are demarcated by setting the threshold of risk. Simulation results testify that the selection of the collision zones and crossing angles affect the collision risk apparently. The results also demonstrate the effectiveness of separation criteria demarcated by 'Equivalent Level of Safety' (ELoS). Statistical analysis for 100 sampled environments shows the reliability of the proposed method, which captured the characteristics of sUAVs and could be utilized for elaborative separation framework in structured low-altitude airspace.

保持安全间隔对于实现无人航空器 (UAV) 的可靠运行至关重要。鉴于与 UAV 相关的碰撞风险日益严重，间隔标准已成为空域设计和避碰策略的基础。然而，大多数现有模型在评估与有人驾驶飞机的统一间隔体积时，并未充分考虑小型无人机 (sUAV) 相遇的特点和空域结构。本文提出了一种基于碰撞风险估计的 sUAV 安全间隔划分方法。首先，根据形状特征确定了五个碰撞区域以确定碰撞。然后，从 3-D 概率密度函数 (PDF) 和总系统误差 (TSE) 的最大值建立了碰撞风险模型。最后，通过设置风险阈值划分了不同相遇场景的最小安全间隔。模拟结果表明，碰撞区域和交叉角度的选择明显影响碰撞风险。结果还证明了通过“等效安全水平”(ELoS) 划分的间隔标准的有效性。对 100 个采样环境的统计分析表明，所提出方法的可信度，该方法捕捉了 sUAV 的特点，可用于结构化低空域的详细间隔框架。

1. Introduction

1. 引言

Unmanned aerial vehicles (UAVs) have been widely deployed in civilian applications due to their economic efficiency and conveniences, such as logistics, facility inspection, and traffic monitoring [1,2]. However, the expansion of these operations has raised imperative concerns about their safety and reliability, i.e., Mid-Air Collision (MAC) with other air traffic [3] and Third-Party Risk (TPR) by ground impact on pedestrians [4, 5] . To help achieve safe and efficient UAS integration into the National Airspace System (NAS), the capacity of separation maintenance is crucial. As a fundamental enabler of system safety, separation requirements have been extensively utilized by abundant research, such as UAV swarm cooperative control [6], task assignment [7], path planning [4,8], low-altitude airspace design [3] and collision avoidance [9, 10] . Meanwhile, the regulatory organizations have mandated the use of collision avoidance systems to mitigate the risk of MAC, and standardized the separation criteria of conflict management systems, e.g., the Federal Aviation Administration (FAA) [11] and the International Civil Aviation Organization (ICAO) [12]. In the current state, quantitative separation criteria not only act as a design target of missions but also act as "measuring sticks" for assessing the goodness of a given drone-specific Detect and Avoid (DAA) system [13], as presented in Fig. 1.

无人机 (UAV) 由于其经济效益和便利性，如物流、设施检查和交通监控 [1,2]，已经在民用领域得到广泛应用。然而，这些业务的扩展引发了对它们的安全性和可靠性的紧迫关注，即与其他航空交通的空中碰撞 (MAC)[3] 和地面撞击行人的第三方风险 (TPR) [4, 5] 。为了帮助实现无人机系统 (UAS) 安全高效地融入国家空域系统 (NAS)，保持间隔的能力至关重要。作为系统安全的基本使能因素，间隔要求已经被大量研究广泛利用，如无人机群协同控制 [6]、任务分配 [7]、路径规划 [4,8]、低空空域设计 [3] 和碰撞避免 [9, 10] 。同时，监管机构已经要求使用碰撞避免系统来减轻 MAC 的风险，并标准化了冲突管理系统之间的间隔标准，例如，联邦航空管理局 (FAA)[11] 和国际民用航空组织 (ICAO)[12]。在当前状态下，定量的间隔标准不仅作为任务设计的目标，还作为评估给定无人机特定的检测与避免 (DAA) 系统良好性的“衡量尺”，如图 1 所示 [13]。

In traditional air transportation system, separation is characterized as the cornerstone with unambiguous standards, e.g., 5 nautical miles (NM) en-route [14] and 3NM in terminal areas for air traffic control [15]. Due to the rarity of MAC in the UAV domain, the quantitative Near MAC (NMAC) acts as a surrogate for a MAC that is intended for incident reporting and investigation of dangerous encounters [16]. Such a definition of 500ft horizontally and 100ft vertically is utilized for the safety modeling of UAV DAA system [13,17], which has been adopted by the Radio Technical Commission for Aeronautics (RTCA). Therefore, the prototype of NMAC provides an off-the-shelf solution for the integration of UAVs into NAS by setting the spatial boundaries between manned aircraft and large UAVs [18,19], especially the Beyond-Visual-Line-of-Sight (BVLOS) operations around airdromes. On this basis, the well clear is characterized as a quantitative state that implies that collision avoidance will likely be unnecessary, as depicted

在传统的航空运输系统中，分离特性被定义为具有明确标准的基石，例如，航路中 5 海里 (NM)[14] 和 3NM 在终端区用于空中交通管制 [15]。由于无人机 (UAV) 领域 MAC 的罕见性，定量的近 MAC(NMAC) 作为 MAC 的替代品，用于事件报告和危险遭遇的调查 [16]。此类 500ft 水平方向和 100ft 垂直方向的定义被用于无人机防撞回避系统 (DAA) 的安全性建模 [13,17]，该定义已被航空无线电技术委员会 (RTCA) 采用。因此，NMAC 原型为无人机集成到国家空域系统 (NAS) 提供了一种现成的解决方案，通过设定有人驾驶飞机和大型无人机之间的空间边界 [18,19]，特别是在机场周边的视距外 (BVLOS) 运行。在此基础上，" 清晰" 被定义为一种定量状态，意味着碰撞回避很可能是不必要的，如图所示

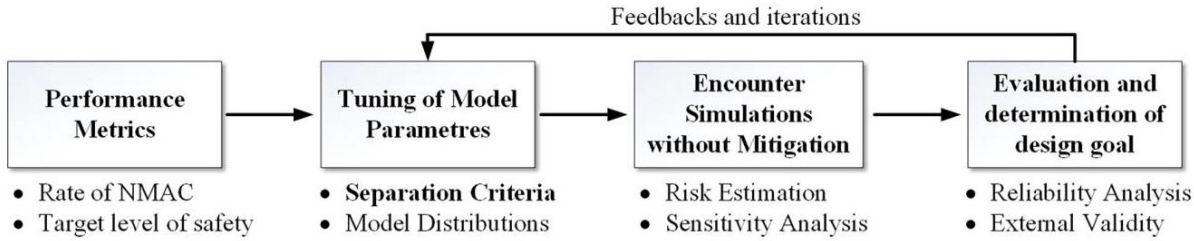

* Corresponding author.
* 对应作者。
E-mail address: zg1991@nuaa.edu.cn (G. Zhong).
电子邮件地址:zg1991@nuaa.edu.cn(G. Zhong)。

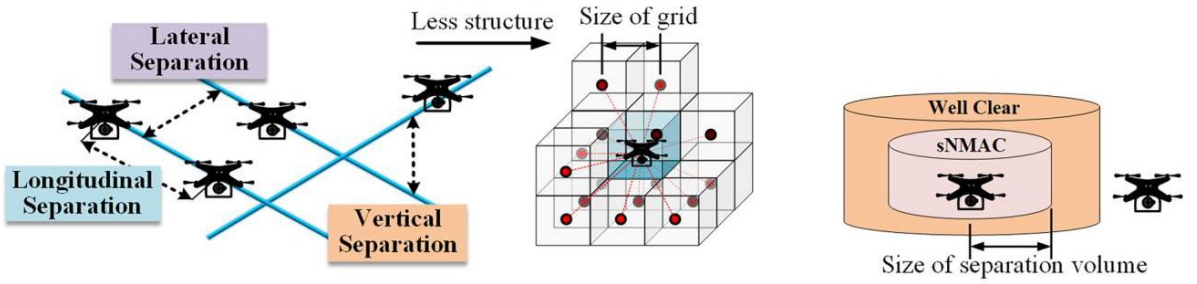

Fig. 2. UAV Separation with and without pre-planned airspace structures.

图 2. 无人机在有和无预先规划空域结构时的分离情况。

in Fig. 2. However, the statistics of UAVs show that the wingspan and height distributions skewed toward smaller dimensions (less than 25ft), supported by FAA aircraft registrations [18, 19] . To avoid overestimating the collision risk for the small UAVs' (sUAVs) encounters, the smaller NMAC (sNMAC) was proposed to enable the generation of a set of metrics used to train and evaluate Airborne Collision Avoidance System X for sUAVs (ACAS sXu) [20,21], e.g., 50 ft/15 ft [13].

如图 2 所示。然而，无人机的统计数据显示，翼展和高度分布倾向于较小的尺寸 (小于 25ft)，由 FAA 飞机注册信息 [18, 19] 支持。为了避免对小无人机 (sUAVs) 遭遇的碰撞风险估计过高，提出了较小的 NMAC(sNMAC)，以生成一组用于训练和评估用于 sUAVs 的空中碰撞回避系统 X(ACAS sXu) 的度量标准 [20,21]，例如，50 英尺/15 英尺 [13]。

Furthermore, the aforementioned separation criteria for UAVs are all utilized to be a stick of in-flight collision avoidance in uncontrolled regions (Class G airspace), without pre-planned airspace structure [22]. It could be insufficient to guarantee that no conflict will happen with online collision resolution only [17]. The difficulty of safely separating UAVs in dense urban airspace can be reduced through the careful design of additional airspace structures as they can minimize complexity and increase throughput [8]. As envisioned by FAA and NASA, the UTM will enable the integrated operations which contain the air geofencing, capacity management and multiple layers of separations, et.al [11]. Several researches have explored the adaptive airspace models on the discrete spatial volume, which have achieved superior performance [4, 23,24]. There is, however, no clear consensus on the type of airspace design that should be implemented, let alone separation requirements

此外，上述用于无人机的分离标准均被用作在不受控制的区域 (G 类空域) 中飞行冲突避免的依据，而无需预先规划的空域结构 [22]。仅依靠在线冲突解决可能不足以保证不会发生冲突 [17]。在密集的城市空域中，通过精心设计额外的空域结构可以降低安全分离无人机的难度，因为它们可以最小化复杂度并提高吞吐量 [8]。正如 FAA 和 NASA 设想的那样，UTM 将使得包含空域围栏、容量管理和多层分离等在内的集成操作成为可能 [11]。已有研究探讨了在离散空间体积上的自适应空域模型，并取得了优越的性能 [4, 23,24]。然而，对于应该实施何种空域设计方案，更不用说分离要求，尚无明确的共识。[3].

The permission for UAV integration into NAS is determined by whether they will behave the same as traditional aviation [25]. Besides, the concept of Equivalent Level of Safety (ELoS) was proposed for UAV [5], which means that the integration of UAVs should not downgrade the safety level of NAS [26]. Based on quantitative threshold of risk in the air transportation system, the criterion is set for separation assurance as Target Level of Safety (TLS), e.g., 10^{-7} accidents per flight hour [27, 28]. Whether the safety criterion is too rigid for sUAVs is still under debate [25]. However, such a clear definition of risk could support the structured airspace design in low altitudes that enable safe and reliable operations. Subsequently, the gap between online collision avoidance and airspace structure poses questions related to hierarchical separations for sUAVs operating in structured airspace.

无人机融入国家空域系统 (NAS) 的许可取决于它们是否能够像传统航空一样表现 [25]。此外，为无人机提出了等效安全水平 (ELoS) 的概念 [5]，这意味着无人机的集成不应降低 NAS 的安全水平 [26]。基于空中运输系统中风险的定量阈值，为分离保障设定了目标安全水平 (TLS) 标准，例如每飞行小时 10^{-7} 起事故 [27, 28]。对于小型无人机 (sUAVs) 来说，安全标准是否过于严格仍在讨论中 [25]。然而，这种对风险的明确定义可以支持在低空进行结构化的空域设计，以实现安全和可靠的运行。随后，在线冲突避免与空域结构之间的差距引发了有关在结构化空域中运行的 sUAVs 分层分离的问题。

1 How to formulate elaborative separation criteria for sUAVs-only encounters, when considering the shape characteristics, outstanding maneuverability and navigation performance, e.g., rotary-wing?

1 如何为仅 sUAVs 相遇制定详尽的分离标准，考虑到形状特性、卓越的机动性和导航性能，例如旋翼机?

2 How to create a compatible separation framework for the design and evaluation of UTM, containing definitions of sNMAC, well clear, and separations of air routes based on the safety criteria in force (ELoS), instead of

real-time collision avoidance only [29]?

如何为无人机交通管理系统 (UTM) 的设计和评估创建一个兼容的分离框架，包含 sNMAC、良好间隔和基于现行安全标准 (ELoS) 的航路分离定义，而不是仅限于实时避障 [29]?

Additionally, the risk-based methodologies emphasize the statistics of trajectory error en route [30], that is inadequate in the UAV domain [31,32]. The concept of Performance Based Navigation (PBN) for sUAVs is under intense research to reveal the influential mechanism of operational capacity on trajectory deviation in urban airspace, as the navigation equipment always maintains a high update rate.

此外，基于风险的方法强调轨迹误差的统计信息在航路上 [30]，这在无人机领域是不充分的 [31,32]。针对小型无人机 (sUAVs) 的性能基础导航 (PBN) 概念正在受到深入研究，以揭示在城市空域中运行能力对轨迹偏差的影响机制，因为导航设备总是保持高更新率。

Consequently, the paper proposes a collision risk estimation model for encounters of small rotary-wing UAVs (omitted as sUAVs below) in low-altitude structured airspace. As illustrated in Fig. 2, we adopt 'ELoS' as the threshold of the separations for well clear and airspace design, and extend them to build a compatible framework with sNMAC. The influential mechanism of trajectory deviation on collision risk is also discussed systematically. Note that the paper focuses on a distance-based separation framework since the time-based separations are infeasible for the size of the air matrix or the width of air routes. Also, the TPR is out of the scope. The main contributions of the paper are summarized.

因此，本文提出了一种小型旋翼无人机 (以下简称 sUAVs) 在低空结构化空域中遭遇的碰撞风险估计模型。如图 2 所示，我们采用'ELoS' 作为良好间隔和空域设计的分离阈值，并将其扩展以构建与 sNMAC 兼容的框架。本文还系统地讨论了轨迹偏差对碰撞风险的影响机制。请注意，本文专注于基于距离的分离框架，因为基于时间的分离对于空气矩阵的大小或航路宽度来说是不可行的。此外，TPR 不在本文讨论范围内。本文的主要贡献如下所述。

1 We propose a separation demarcation method for sUAVs in structured low-altitude airspace. Align with the safety criterion in force, the separation criteria could be utilized as a metric for the design and evaluation of air routes, the capacity of separation maintenance, and collision avoidance systems. Also, the framework of hierarchical separations is established to provide benchmarking for low-altitude air transportation systems in the future.

本文提出了一种在结构化低空空域中为 sUAVs 划分分离界限的方法。符合现行安全标准，分离标准可用作航路设计及评估、分离保持能力和避障系统的度量。此外，建立了分层分离框架，以期为未来的低空交通系统提供基准。

2 We develop a collision risk model for sUAVs considering the shape characteristic, maneuverability, and navigation performance. The collision probability estimations are conducted by the sequence of events and 3-D probability calculation, which provides more safety and reliability margin for risk assessment of sUAVs' operations.

我们开发了一个考虑形状特性、机动性和导航性能的 sUAV 碰撞风险模型。通过事件序列和 3-D 概率计算进行碰撞概率估计，这为 sUAV 操作的风险评估提供了更大的安全性和可靠性余地。

3 We conduct systematical sensitivity analysis of trajectory error, collision shape and encountering scenarios, which provides the reference for precise design of low-altitude airspace, e.g., selection of crossing angles and navigation performance. Due to the high-update rate of navigation in UTM, the supremum of the deviation constraints is also determined by the modeling of 3-D Gaussian distribution.

我们对轨迹误差、碰撞形状和遭遇场景进行了系统的敏感性分析，这为精确设计低空空域提供了参考，例如选择交叉角度和导航性能。由于 UTM 中导航的高更新率，偏差约束的上限也由 3-D 高斯分布的建模确定。

4 We analyze the discrepancy of different types of collision zones. Apart from our previous work [33], we redefine the sNMAC volume based on the minimum envelope of the sUAV to investigate the mechanism of shape characteristics on separations in different encountering scenarios. The computational time of risk estimation is also considered to illustrate the superiority-inferiority of them.

我们分析了不同类型碰撞区域的差异。除了我们之前的工作 [33]，我们还基于 sUAV 的最小包络重新定义了 sNMAC 体积，以研究形状特性在不同遭遇场景中对分离机制的影响。同时，也考虑了风险估计的计算时间，以说明它们的优势和劣势。

Based on continued maturation of UTM, the work is intended to provide the supplement of current separation criteria with more elaborative methodology and applications, such as RTCA SC-147 [21], and SC-228 [34]. Along with the need of multi-layer separation framework proposed by FAA [11], the work provides the quantitative method to evaluate and demarcate the hierarchical standardization. Furthermore, the collision risk model with 'ELoS' could be compatible with the Specific Operations Risk Assessment (SORA) proposed by Joint Authorities for Rulemaking of Unmanned Systems (JARUS) [35]. The remainder of this paper is organized as follows. Section 2 presents the related works. In Section 3, the sNMAC volume is established by shape characteristics with 5 types. In Section 4, the method of separation demarcation is proposed by estimation of collision risk. In Section 5, Numerical simulations are conducted to demarcate the separations of different encountering scenarios, and a

comparison analysis is also presented. In Section 6, a compatible separation framework for sUAV is proposed with the discussion of future works. Section 7 concludes the research findings in the paper.

基于持续成熟的 UTM(无人交通管理系统)，本工作的目的是提供对当前分离标准的补充，采用更详尽的方法和应用，例如 RTCA SC-147 [21] 和 SC-228 [34]。随着美国联邦航空局 (FAA)[11] 提出的多层分离框架需求，本工作提供了定量方法来评估和划分层级标准化。此外，带有'ELoS' 的碰撞风险模型可以与由无人系统规则制定联合机构 (JARUS)[35] 提出的特定操作风险评估 (SORA) 兼容。本文其余部分的组织结构如下。第 2 节介绍相关工作。第 3 节通过 5 种形状特征建立 sNMAC(最小安全间隔) 体积。第 4 节提出了通过碰撞风险评估来划分分离的方法。第 5 节进行了数值模拟，以划分不同遭遇场景的分离，并进行了比较分析。第 6 节提出了适用于 sUAV(小型无人机) 的兼容分离框架，并讨论了未来的工作。第 7 节总结了本文的研究成果。

2. Literature review

2. 文献综述

The essentials of separation assurance for UAVs are to resolve conflicts through an established threshold of distance or time [36]. By the overview of the application scenarios, the current researches on UAVs separation requirement focus on two aspects. The first aspect is from the separation in unstructured airspace to realize real-time path planning for multi-UAVs, which corresponds to DAA functions, i.e., well-clear and collision avoidance [19,37]. The second aspect is from the separations in structured airspace, which is path planning cooperating with pre-planned types of airspace, e.g., air matrix [4], air geofencing [24], and so on, that is strategic trajectory-based collision avoidance. Based on the safety metric of ELoS, the commonly used probabilistic collision risk models in air traffic management are discussed. Furthermore, the researches on the PBN concept in UTM are summarized in this section which determines the flight path precision of UAVs.

无人机分离保障的关键是通过对距离或时间的既定阈值来解决冲突 [36]。通过应用场景的概述，当前关于无人机分离要求的研究主要集中在两个方面。第一个方面是从非结构空域中的分离来实现多无人机的实时路径规划，这对应于 DAA 功能，即清晰分离和避撞 [19,37]。第二个方面是结构空域中的分离，这是与预先计划的空域类型协同的路径规划，例如，空气矩阵 [4]、空中地理围栏 [24] 等，即基于战略轨迹的避撞。基于 ELoS 的安全指标，本节讨论了空中交通管理中常用的概率碰撞风险模型。此外，本节还总结了无人机交通管理 (UTM) 中 PBN 概念的研究，该概念决定了无人机飞行路径的精度。

2.1.UAV separation assurance

2.1. 无人机分离保障

2.1.1. Separations in unstructured airspace

2.1.1. 非结构空域中的分离

The capabilities of the DAA system on board are characterized as the core of the authorization to enter the NAS [11,22]. In 2013, the UAS Executive Committee (EXCOM) Science and Research Panel (SARP) was charged with making a recommendation for a quantitative definition of well clear to support large UAVs, that was adopted by RTCA Special Committee-228 with a small modification (DO-365) [34,38]. Such a well-clear volume was defined by the distance separation of $4000\text{ft}/\ \pm 450\text{ft}$ and modified time τ_{mod} to spatial volume of 35 s . Under the researches major from Massachusetts Institute of Technology Lincoln Laboratory (MIT LL) in the past decade, methods have been well-established to evaluate well clear volume for UAVs encountering with manned aircraft based on the relative encounter geometry and the performance characteristics of each aircraft [18,37,38]. Align with MIT LL, NASA also offered to provide formal methods analysis of the different equations used to define UAS Well Clear [39]. Edward has summarized five existing definitions of well clear in different applicable scenarios [18], e.g., $2000\text{ft}/\ \pm\ 250\text{ft}$ adopted by American Society of Testing Materials Committee F-38(ASTM F-38) [40] and minimum operational performance standards published by RTCA SC-147 [21], $2200\text{ft}/\ \pm\ 450\text{ft}$ adopted by SC-228 with applicable UAS still being validated $[34, 38]$. As the safety and operational suitability not dependent on τ_{mod} , it may not be necessary to conduct the extra time-based separation [41].

DAA 系统的能力在机上表现为进入国家空域授权的核心 [11,22]。2013 年，无人机系统执行委员会 (EXCOM) 科学与研究小组 (SARP) 受命就为大型无人机提供支持的“清晰空间”的定量定义提出建议，该建议经 RTCA 特别委员会-228 稍作修改后采纳 (DO-365)[34,38]。这样一个清晰空间的体积由 $4000\text{ft}/$

±450ft 的距离分离和修改时间 τ_{mod} 来确定空间体积的 35 s 。在麻省理工学院林肯实验室 (MIT LL) 过去十年的研究基础上，已经建立了基于相对遭遇几何学和每架飞机性能特征评估无人机与有人机遭遇时清晰空间体积的方法 [18,37,38]。与 MIT LL 保持一致，NASA 也提供对不同方程式用于定义无人机清晰空间的正式方法分析 [39]。Edward 总结了在不同应用场景下现有的五个清晰空间定义 [18]，例如，美国测试与材料协会委员会 F-38(ASTM F-38) 采用的 2000ft/ ± 250ft [40] 以及 RTCA SC-147 发布的最低运行性能标准 [21]，SC-228 采用的 2200ft/ ± 450ft，适用于仍在验证中的无人机 [34, 38] 。由于安全性和运行适用性不依赖于 τ_{mod} ，因此可能无需进行额外的时间分离 [41]。

NMAC with 500ft/100ft is adopted as the baseline to determine the aforementioned well-clear volumes through Monte Carlo simulation [37,38]. Then, based on the statistics generated by MIT LL encountering models, the self-separations (well clear) are determined by conditional probability P (NMAC|LossofWellClear) with a probabilistic threshold, e. g., 5 % set primarily by RTCA [37]. To enclose most of the collision system, the metric was down selected by 1.5% and finally adjusted to 2.2 % [38,41]. Also, NMAC serves as a safety metric to evaluate the efficiency of DAA through the proximity rate mitigated by traffic alert [13,38], and the online guidance algorithms for multi-UAVs in free flights [9,10,17]. In recent years, the dramatic expansion of sUAVs' market precipitated similar definitions for them. Some recommendations of well clear are provided for sUAVs under 55 pounds with the same metric of NMAC, especially when encountering with manned aircraft [19,22]. Considering the wingspan of sUAVs, Weinert recommended 10% NMAC along with other possible candidates, 4.75% , and 5.75% [19]. However, it could be unreasonable to be utilized in sUAVs-only encounters. To overcome this, Weinert defined the sNMAC for sUAVs with wingspan less than 25ft [13]. Additionally, considering the maneuverability and response time, the directional safety bound for rotary-wing UAVs is proposed to support conflict detection and resolution in real time [42].

使用 500ft/100ft 的 NMAC 被采用作为基线，通过蒙特卡洛模拟 [37,38] 确定上述的清晰空间体积。然后，基于由 MIT LL 遭遇模型生成的统计数据，通过条件概率 P (NMAC|LossofWellClear) 以及主要由 RTCA [37] 设置的概率阈值 (例如，5%)，确定自我分离 (清晰) 条件。为了包含大多数的碰撞系统，该度量通过 1.5% 进行筛选，并最终调整至 2.2% [38,41]。此外，NMAC 作为安全度量，用于评估通过交通警报缓解的接近率来衡量 DAA 的效率 [13,38]，以及自由飞行中多无人机 (UAV) 的在线引导算法 [9,10,17]。近年来，小型无人机 (sUAVs) 市场的急剧扩张促使了对它们的类似定义。为重量小于 55 磅的 sUAVs 提供了一些建议的清晰空间，使用与 NMAC 相同的度量，特别是在与有人驾驶飞机遭遇时 [19,22]。考虑到 sUAVs 的翼展，Weinert 建议 10% NMAC 以及其他可能的候选者 4.75% 和 5.75% [19]。然而，在仅 sUAVs 相遇的情况下使用这可能是不合理的。为了克服这一点，Weinert 为翼展小于 25ft 的 sUAVs 定义了 sNMAC [13]。此外，考虑到机动性和响应时间，提出了适用于旋翼无人机的方向安全边界，以支持实时冲突检测和解决 [42]。

2.1.2. Separations in structured airspace

2.1.2. 结构化空域中的间隔

Driven by initiatives of government and industry, some proposals have been provided to design low-altitude airspace [11]. As summarized in Ref. [3], airspace models in UTM can be divided into full mix (free flight), layers, zones, and tubes, ranking by complexity. Tube-type airspace can be considered an appropriate model for rotary-wing UAVs due to its high safety level [23]. Recent studies pay attention to discrete 3-D air matrix modeling for low-altitude airspace which is a subtype of tubes. Aligned with sky-lanes and corridors proposed by NASA, the air matrix reduces the collision risk strategically through static safe separation with other UAVs in adjacent air blocks [4,43], depicted in Fig. 2. Subsequently, 4-D trajectory optimization is conducted with different objectives by flight schedules and trajectory adjustment [8,36,43]. Existing models like heuristic algorithms like A* [36], and swarm-based heuristic methods [44].

在政府和企业倡议的推动下，已经提出了某些设计低空空域的提案 [11]。正如参考文献 [3] 中总结的，UTM 中的空域模型可以分为完全混合 (自由飞行)、层次、区域和管道，按复杂性排序。管道型空域由于其高安全级别 [23]，可以被认为是旋翼无人机的一个合适模型。近期研究关注于低空空域的离散 3-D 空气矩阵建模，这是管道的一个子类型。与 NASA 提出的天空通道和走廊对齐，空气矩阵通过与其他无人机在相邻空气块中的静态安全间隔来战略性地降低碰撞风险 [4,43]，如图 2 所示。随后，根据飞行计划和轨迹调整 [8,36,43]，进行了以不同目标进行的 4-D 轨迹优化。现有模型包括启发式算法如 A* [36]，以及基于群体的启发式方法 [44]。

However, the researches always take a fixed size of air block, e.g., 100 m∗100 m∗30 m [4, 36] , 30 m∗30 m [43] . To overcome the inefficiency utilization of airspace, Dai designed the adaptive air blocks influenced by the GPS-induced tracking deviation [45]. Base on the GPS precision threshold, Delamer discussed different grid size for path planning [46]. And Shao proposed the similar structure through dynamic and configuration of sUAVs [23].

Additionally, the dynamic air geofencing was conducted to keep separations by rectangular volumes wrapping the track, also with the fixed separations set initially [24].

然而，这些研究总是采用固定大小的空气块，例如 $100\ \mathrm{m} * 100\ \mathrm{m} * 30\ \mathrm{m}$ [4, 36] , $30\ \mathrm{m} * 30\ \mathrm{m}$ [43] 。为了克服空域利用效率低下的问题，Dai 设计了受 GPS 引入的跟踪偏差影响的自适应空气块 [45]。基于 GPS 精度阈值，Delamer 讨论了路径规划的不同网格大小 [46]。Shao 通过动态配置小型无人机 (sUAVs) 提出了类似结构 [23]。此外，进行了动态空域地理围栏，以保持通过围绕轨迹的矩形体积包裹的分离，初始时也设置了固定的分离 [24]。

2.2. Collision risk models

2.2. 碰撞风险模型

Since there is no consensus that airspace design implemented in low-altitude airspace [3], the conceive could refer from traditional Air Traffic Management (ATM) consistent with ELoS. For the top layer of the ATM design, the collision risk models aims to estimate the rate or the probability of the collision, including the Reich model [47], Intersection model [48], summarized in Ref. [49]. Through the constraints and modeling purposes of them, the methodologies could be categorized by the collision shapes which is established by the realistic size of fuselage for collision determination, e.g., parallelepiped shape, cylinder, or ellipsoid [49]. While the region is predesigned to express the physical space occupied by intruders, the stochastic process of collision is modelled as the probability distribution function derived by data-driven or randomized motion e.g., double-exponential function and Gaussian distribution [16, 30] .

由于在低空空域实施空域设计方面没有共识 [3]，该概念可以参考与传统空中交通管理 (ATM) 一致的 ELoS。在 ATM 设计的顶层，碰撞风险模型旨在估计碰撞的速率或概率，包括 Reich 模型 [47]、交叉模型 [48]，在文献 [49] 中进行了总结。通过它们的约束和建模目的，这些方法可以根据碰撞形状进行分类，该形状是由机身实际尺寸建立的碰撞确定，例如，长方体形状、圆柱体或椭球体 [49]。而该区域被预设为表示入侵者占据的物理空间，碰撞的随机过程被建模为概率分布函数，该函数由数据驱动或随机运动导出，例如，双指数函数和高斯分布 [16, 30] 。

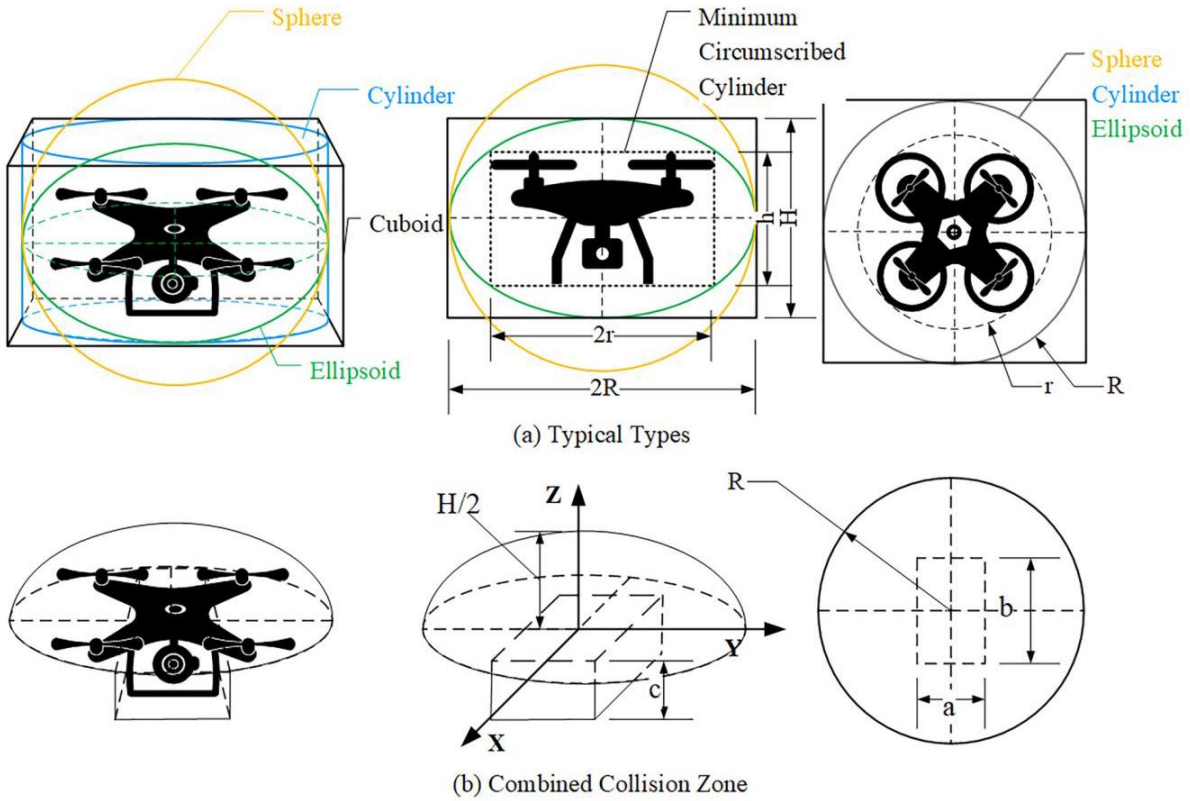

Fig. 3. Collision zones.
图 3. 碰撞区域。

The parallelepiped zone is early adopted by Reich model which was developed to determine the longitudinal, lateral, and vertical separations [50,51]. It was conducted conveniently since the collision probability is calculated independently from each direction. Nowadays, to improve the calculation accuracy and applicability, cylinder-based model was proposed through linear transformation [52]. While extending to sUAV domain, Zou established different collision zones for sUAV and used the Laguerre polynomial to expand the Gaussian distribution [33], thereby simplifying the approximate 3-D probability integral calculation. Differing from the few levels change in cruising, 3-D methodologies will be more suitable for sUAVs operations. Another aspect of improvement is from the workflow optimization with dynamics and uncertainty captured [30]. Considering the specific geometry and DAA functions on board, Zhang assessed collision risk of the airspace flow corridor through the sequence of events [16].

长方体区域早期被 Reich 模型采用，该模型用于确定纵向、横向和垂直间隔 [50,51]。由于碰撞概率是从每个方向独立计算的，因此操作方便。如今，为了提高计算精度和适用性，提出了基于圆柱体的模型，通过线性变换 [52]。在扩展到小型无人机 (sUAV) 领域时，Zou 为 sUAV 建立了不同的碰撞区域，并使用 Laguerre 多项式展开高斯分布 [33]，从而简化了近似三维概率积分的计算。与巡航中少数级别的变化不同，三维方法更适合 sUAV 的操作。另一个改进方面是工作流程的优化，其中包含了动态和不确定性的捕捉 [30]。考虑到具体的几何形状和机载防撞功能，Zhang 通过事件序列评估了空域流量走廊的碰撞风险 [16]。

2.3.PBN concept in UTM

2.3. UTM 中的 PBN 概念

In terms of collision risk assessment, trajectory estimation and propagation are the basis [53]. Often the stochastic process according to which aircraft motion is modelled to be stationary and Gaussian, which is validated by empirical studies and statistics in manned aviation [30, 49,54]. While the determination and enforcement of separation minima to sUAV in a given airspace depends on the total system error (TSE) [32]. The TSE complies with the Required Navigation Performance (RNP) which captures the true position offset probability of the aircraft from its intended track.

在碰撞风险评估方面，轨迹估计和传播是基础 [53]。通常，根据经验研究和有人驾驶航空的统计数据，飞机运动的随机过程被建模为静止和高斯过程 [30, 49,54]。而在给定空域内为小型无人机 (sUAV) 确定和执行最小间隔距离取决于总系统误差 (TSE)[32]。TSE 符合所需导航性能 (RNP)，该性能捕捉了飞机实际位置偏移其预定航道的概率。

Fellner categorized the TSE into path definition error (PDE), navigation system error (NSE), and flight technical error (FTE) [55]. Subsequently, flight experiments and statistical analysis are conducted to determine the optimal fitting distribution [56]. However inadequate UAS air corridors have been implemented that could be used for PDE analysis [3]. And NSE depends on the navigation performance in dense urban areas [57]. For instance, the change in altitude may have a significant influence on the performance of navigation equipment [31]. Pang proposed an evaluation framework for the determination of FTE by investigating flight trajectory error deviations, which determine the significance level and supports the future path definition of tube-based routes in urban airspace [32]. However, the determination of the TSE distribution needs to be instantaneous to meet the requirement of efficiency. As a result, the static TSE distribution could be utilized by setting the supremum to meet the accuracy requirement [58].

Fellner 将 TSE 分为路径定义误差 (PDE)、导航系统误差 (NSE) 和飞行技术误差 (FTE)[55]。随后，进行了飞行实验和统计分析以确定最优拟合分布 [56]。然而，尚未实施足够的小型无人机空中走廊，这些走廊可用于 PDE 分析 [3]。而 NSE 取决于密集城市区域的导航性能 [57]。例如，高度的变化可能对导航设备的性能产生重大影响 [31]。Pang 提出了一个评估框架，通过研究飞行轨迹误差偏差来确定 FTE，这决定了显著性水平，并支持未来基于管道的城市空域航路的路径定义 [32]。然而，确定 TSE 分布需要即时进行以满足效率要求。因此，可以通过设置最大值来使用静态 TSE 分布以满足精度要求 [58]。

Overall, separation requirements focus on real-time collision avoidance system for UAVs vs manned aircraft. There is rare research on separations for sUAVs-only encounters, especially the definition of well clear. Meanwhile, few studies have explored the collision risk assessment and separation criteria for low-altitude airspace design, let alone the clear definition of a cooperative separation framework containing both. The lack of such an essential safety metric will fail to support regulatory needs and standardization activities for acceleration of UAV integration. As the baseline need to be structured for sUAVs in low-altitude airspace with a quantitative metric, the probabilistic collision risk models in traditional aviation offer a feasible solution to redefine separations for sUAVs. The cooperative development of pre-flight and in-flight standardization will help to achieve the optimal balance between operational efficiency and safety.

总的来说，分离要求集中在无人机与有人驾驶飞机的实时避障系统。对于仅涉及小型无人机的相遇，

尤其是“清晰间隔”的定义，研究较少。同时，很少有研究探讨低空空域设计中碰撞风险评估和分离标准，更不用说包含两者的合作分离框架的明确定义了。这种基本安全指标的缺失将无法满足监管需求和无人机集成加速的标准化活动。由于需要为低空空域中的小型无人机构建一个具有定量指标的基础，传统航空中的概率碰撞风险模型为重新定义小型无人机的间隔提供了一个可行的解决方案。预先飞行和飞行中的标准化合作将有助于在运营效率和安全性之间实现最佳平衡。

3. Collision zone

3. 碰撞区域

NMAC is predesigned with a cylindrical volume to be a surrogate of MAC with a uniform value. Currently, the size of sNMAC is generated through the set of stochastic encounters with P (MAC | NMAC) of 10% [13], or 1 % [18]. Hence, there is no clear definition of sNMAC in structured airspace. Considering the characteristics and the wingspan of individuality, we established the collision zone by geometric extension of fuselage in the section. The redefined the collision zone is characterized as a 'extreme case' of sNMAC. In this event, the rationale is that the MAC can be determined by the overlap of the zones when the relative positions of the sUAVs are known.

NMAC 被预设为一个圆柱体，作为具有均匀值的 MAC 的替代。目前，小型 NMAC 的大小是通过一组随机相遇的 P (MAC | NMAC) 的 10% [13]，或者 1 % [18] 生成的。因此，在结构化空域中没有小型 NMAC 的明确定义。考虑到个体特征和翼展，我们通过机身部分的几何扩展建立了碰撞区域。重新定义的碰撞区域被特征化为 sNMAC 的“极端情况”。在这种情况下，逻辑是当小型无人机的相对位置已知时，MAC 可以通过区域的重叠来确定。

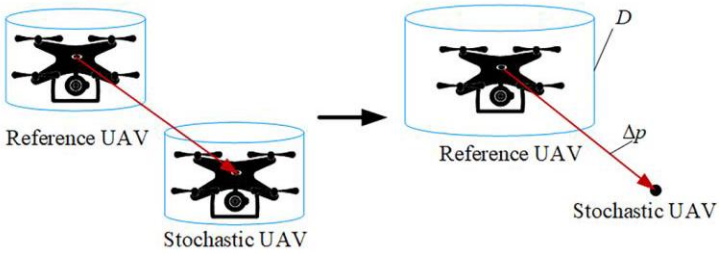

Fig. 4. Superimposed collision zone.
图 4. 叠加的碰撞区域。

3.1. Types

3.1. 类型

The typical collision zone of the sUAV is modelled as regular shapes, e.g., cuboid, cylinder, sphere, and ellipsoid [33], The safety boundaries conform to the characteristics of the fuselage, that provides convenience for subsequent calculations of collision probability. Supposing that there is a sUAS whose airframe is kept straight-and-level, and its height is h and length is $2r$, then it can be put into a cylinder that exactly encloses the airframe. We assume the circumscribed ellipsoid can give sUAS enough space for maneuvering, e.g., pitch and roll. The parameters of the collision zone can be computed as Eq. (1).

小型无人机的典型碰撞区域被建模为规则形状，例如，长方体、圆柱体、球体和椭球体 [33]，安全边界符合机身的特点，这为后续计算碰撞概率提供了便利。假设存在一个小型无人机系统，其机身保持水平直飞状态，其高度为 h ，长度为 $2r$ ，则可以将其放入一个恰好包围机身的圆柱体中。我们假设外接椭球体能够为小型无人机提供足够的空间进行机动，例如俯仰和横滚。碰撞区域的参数可以按照公式 (1) 计算。

$$V_{re}(H,R)=\frac{2\pi}{3}HR^2-\pi hr^2=\frac{4\pi r^2H^3}{3\left(H^2-h^2\right)}-\pi hr^2 \tag{1}$$

Where $V_{re}(H,R)$ is the residual volume between minimum circumscribed cylinder and ellipsoid, depicted in Fig. 3. Due to $d\left(V_{re}\right)/dH=0$, the basic parameters of the collision zones can be obtained that $H=$

其中 $V_{re}(H,R)$ 是最小外接圆柱体和椭球体之间的剩余体积，如图 3 所示。由于 $d\left(V_{re}\right)/dH=0$ ，可以获得碰撞区域的基本参数 $H=$ 。$\sqrt{3}h, R=\sqrt{3}r.$

To provide a comparative analysis, it is necessary to establish a collision zone that conforms to the appearance of the sUAV mostly. Assuming that the sUAV consists of fuselage and the payload for tasks, e. g., photography, logistics. Then, the new shape is represented by a combination of a semi ellipsoid set above and a cuboid, where the size of the payload is $a \times b \times c$. After that, we obtain a new collision zone which reduces the origin volume with a certain safety margin. The semi ellipsoid equation is as follows.

为了进行对比分析，有必要建立一个与小型无人机外观相符的碰撞区域。假设小型无人机由机身和用于任务的有效载荷组成，例如摄影、物流。那么，新形状由一个半椭球体和一个长方体的组合表示，其中半椭球体位于上方，有效载荷的尺寸为 $a \times b \times c$。之后，我们得到一个新的碰撞区域，该区域在一定的安全边际内减少了原始体积。半椭球体的方程如下。

$$\frac{x^2 + y^2}{R^2} + \frac{4z^2}{H^2} = 1 \; z > 0 \tag{2}$$

It should be noted that the reduction of the volume could be unreasonable or 'extreme', since the maneuverability of sUAVs may tend to be uncontrollable with uncertainties. But it still provides the baseline when assessing the collision risk, and could be adopted by intelligent UTM in the future. The superior and interior of different shapes will be discussed below.

应该注意的是，体积的减少可能是不合理或“极端”的，因为小型无人机的机动性可能因不确定性而变得难以控制。但它在评估碰撞风险时仍提供了基线，并且将来可能被智能空管系统采用。下面将讨论不同形状的上部和内部。

3.2. Superimposed collision zone

3.2. 叠加碰撞区域

Once the type of collision zone is selected, the judgement of the MAC is conducted by superimposed the collision zones of two objects. The simplification is adopted from Reich model [47], and has been widely used in relevant researches [33,49]. In this case, the superposed collision zone of the two objects can be assigned to either of the two, and then the other one can be regarded as a point, depicted in Fig. 4.

选择碰撞区域类型后，通过叠加两个物体的碰撞区域来进行 MAC 的判断。这种简化采用了 Reich 模型 [47]，并在相关研究中得到了广泛应用 [33,49]。在这种情况下，两个物体的叠加碰撞区域可以指定给其中任意一个，然后另一个可以被视为一个点，如图 4 所示。

Therefore, a new definition of collision can be obtained that if the point enters the superposed collision zone, we declare that a collision has happened. If D is the superposed collision zone and Δp is the relative position, the event of collision can be represented by an indicator function

因此，可以获得一个新的碰撞定义，即如果点进入叠加碰撞区域，则我们宣布发生了碰撞。如果 D 是叠加碰撞区域，Δp 是相对位置，那么碰撞事件可以用一个指示函数来表示

$$I_D(\Delta p) = \begin{cases} 1 & \Delta p \in D \\ 0 & \Delta p \notin D \end{cases} \tag{3}$$

4. Methodology

4. 方法论

In this section, the demarcation method is proposed for sUAV separation criteria in structured airspace by collision risk estimation. Depicted in Fig. 5, the workflow consists of three parts. Firstly, orient to the sequence of collision event and stochastic process, the paper establishes the collision risk model through the 3-D probability density function. Secondly, the supremum of TSE is determined to ensure the instantaneous calculation through sensitivity analysis of trajectory deviation. Finally, the 'ELoS' is used as the threshold of risk assessment to demarcate the minimum safe separations for different encountering scenarios.

在本节中，提出了基于碰撞风险估计的 sUAV 在结构化空域中的分离标准划分方法。如图 5 所示，工作流程包括三个部分。首先，本文面向碰撞事件序列和随机过程，通过三维概率密度函数建立了碰撞风险模型。其次，通过轨迹偏差的敏感性分析确定了 TSE 的最大值，以确保瞬时计算。最后，使用'ELoS'作为风险评估的阈值，为不同的遭遇场景划分最小安全间隔。

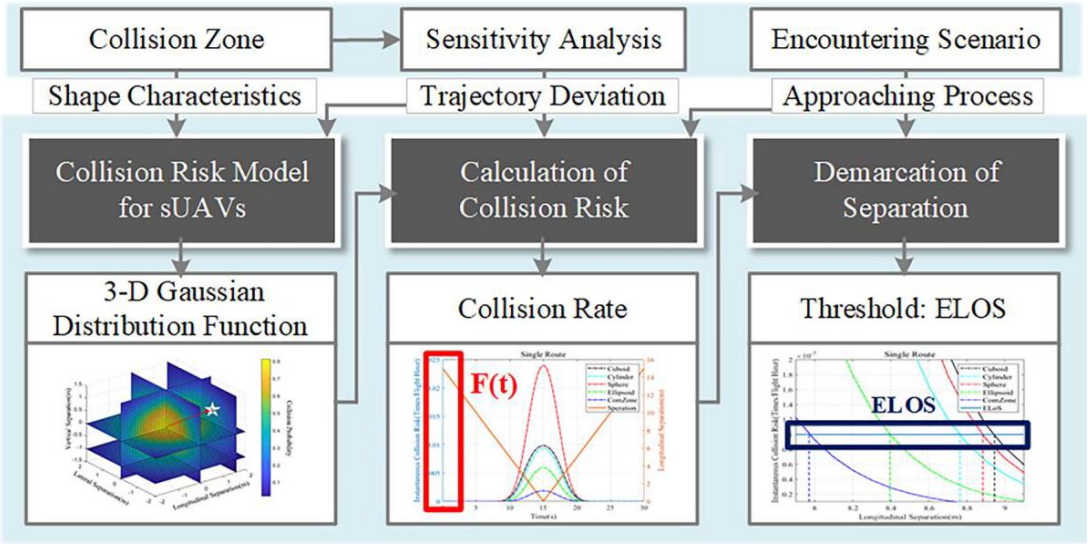

Fig. 5. Schematic overview of the demarcation method of safety separations.
图 5. 安全间隔划分方法的示意图。

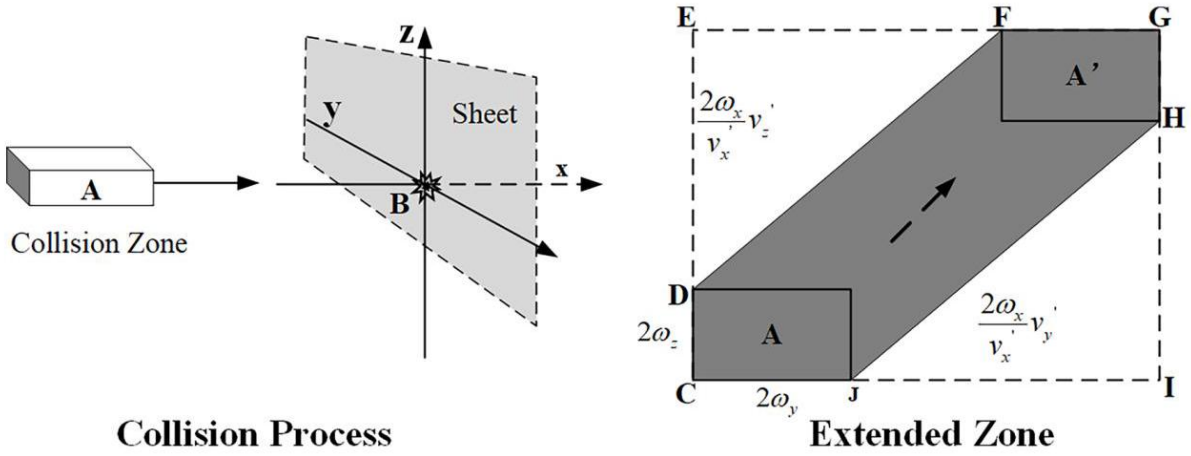

Fig. 6. Event model.
图 6. 事件模型。

4.1. Assumptions and limitations

4.1. 假设和限制

Considering the application scenarios of the model and characteristics of UAV operations, some assumptions and limitations are proposed.

考虑到模型的应用场景和无人机操作的特点，提出了一些假设和限制。

1 We assume that the flight track of each sUAV is independent of others, which operated by an integrated platform. And the trajectory deviation can be simplified as a probability distribution with sUAVs in tube-type air routes [33].

1 我们假设每个 sUAV 的飞行轨迹独立于其他轨迹，这些轨迹由一个集成平台操作。并且轨迹偏差可以简化为概率分布，sUAVs 在管型航线中 [33]。

2 The separations demarcated in the paper correspond to the well clear volume and the width of air routes by unmitigated collision risk [13, 19], which means the dangerous approach or adjacent will not trigger the collision avoidance system or controlled by ATM.

文章中划分的间隔对应于无缓解碰撞风险下的清晰体积和航线宽度 [13, 19]，这意味着危险接近或相邻不会触发避碰系统或由空中交通管制控制。

3 We assume that the sUAVs fly with constant speed and directions set preliminarily in each time period, align with the structured air routes (e.g., single route, parallel routes).

我们假设小型无人机 (sUAVs) 以恒定速度飞行，并在每个时间段内预设方向，与结构化航线 (例如，单一航线、平行航线) 对齐。

To avoid over-simplification, the relevant uncertainties are captured by the conservative principle of risk assessment. Besides, the complicated matter is made to be tractable with reasonable safety margin. conditional probability that B exists in the extended collision zone Additionally, the collision is regarded as two unsafe events.

为了避免过度简化，相关不确定性通过风险评估的保守原则来捕捉。此外，通过合理的安全生产距离，使复杂问题变得可处理。条件概率指的是 B 存在于扩展碰撞区域中的情况。另外，碰撞被视为两个不安全事件。

Considering of the event sequence of separation loss, let F_n (LoWC) denotes the rate of loss of well clear, $P_n\left(MAC \mid LoWC\right)$ denotes the conditional probability of MAC when the self-separations cannot be maintained. Then, the $F\left(SC\right)$ can be computed as

考虑分离损失的事件序列，令 F_n (LoWC) 表示失去清晰间隔的速率，$P_n\left(MAC \mid LoWC\right)$ 表示当自身间隔无法维持时 MAC 的条件概率。那么，$F\left(SC\right)$ 可以计算为

$$F_n\left(SC\right) = F_n\left(LoWC\right) \cdot P_n\left(MAC \mid LoWC\right) \tag{5}$$

Besides, with the extended trajectory, the $P_n\left(Ex \mid SC\right)$ can be computed as the product of the collision probability of two directions in the sheet and the extra terms. For an instance

此外，考虑到扩展轨迹，$P_n\left(Ex \mid SC\right)$ 可以计算为板面上两个方向的碰撞概率与额外项的乘积。例如

$$P_{\text{lon}}\left(Ex \mid SC\right) = P_{\text{lat}}\left(MAC\right) P_{\text{ver}}\left(MAC\right) \Gamma_{\text{lat}} \Gamma_{\text{ver}} \tag{6}$$

Where, Γ_{ver} denotes the first approximation of the proportion in lateral dimension [50], which is calculated as

其中，Γ_{ver} 表示横向维度比例的第一次近似 [50]，其计算方式为

$$P_{\text{ver}}\left(MAC\right) = \int_{-\infty}^{\infty} f\left(v_y'\right) \int_{v-H}^{v+H} f\left(v_z'\right) dv_y' dv_z' \cong P_{\text{ver}}\left(MAC\right)\left(1 + \frac{2v_z'\omega_x}{2v_x'\omega_z}\right) \tag{7}$$

Γ_{lat} is defined in the same way. Therefore, the collision risk in the longitudinal direction can be expressed as

Γ_{lat} 以同样的方式定义。因此，纵向方向的碰撞风险可以表示为

$$F_{\text{lon}} = 2R\left(O\right) \cdot F_{\text{lon}}\left(LoWC\right) \cdot P_x\left(MAC \mid LoWC\right) \cdot P_{\text{ver}}\left(MAC\right) \cdot \left(1 + \frac{2v_z'\omega_x}{2v_x'\omega_z}\right) \cdot P_{\text{lat}}\left(MAC\right) \cdot \left(1 + \frac{2v_y'\omega_x}{2v_x'\omega_y}\right) \tag{8}$$

4.2. Model establishment

4.2. 模型建立

This stochastic process of collision is modelled based on the concept of event sequence which is one of the generalized Reich model [59]. The main character of the Event model is the application of a separate sheet to capture the instantaneous process of collision, making the better feasibility under the influence of complex factors in operation [16,50]. The sheet refers to a plane in body coordination of B. Let $v_i'\left(x, y, z\right)$ denotes relative velocities, $\omega_i\left(x, y, z\right)$ denotes the superimposed collision zone, as shown in Fig. 6. The longitudinal collision process between sUAVs can be equivalent to the collision zone crossing the sheet to form an extended collision zone. At this time, if B exists in the extended collision zone, it is considered that the collision happens.

这种基于事件序列概念的碰撞的随机过程被建模，事件序列是广义 Reich 模型 [59] 之一。事件模型的主要特点是对单独表格的应用，以捕捉碰撞的瞬时过程，使得在操作中受复杂因素影响下的可行性更好 [16,50]。这里的表格指的是 B 体坐标系中的一个平面。令 $v_i'\left(x, y, z\right)$ 表示相对速度，$\omega_i\left(x, y, z\right)$ 表示如图 6 所示的叠加碰撞区域。sUAV 之间的纵向碰撞过程可以等效为碰撞区域穿越表格形成扩展碰撞区域。此时，如果 B 存在于扩展碰撞区域内，则认为发生了碰撞。

The directional collision risk F_n ($n =$ lon, lat, ver) (collisions per flight hour) can be written as

方向碰撞风险 F_n ($n =$ lon, lat, ver) (每飞行小时的碰撞次数) 可以写成

$$F_n = 2F_n\left(SC\right) \cdot P_n\left(Ex \mid SC\right) \tag{4}$$

where $F(SC)$ denotes the rate of Sheet-Crossing (SC), $P(Ex \mid SC)$ denotes the While the cylinder zone was proposed to reduce the origin volume of cuboid, $R(O)$ represents the characteristics of the specific shape calculated by the ratio of the area of the extended trajectory to the area of the sheet [60].

其中 $F(SC)$ 表示表格穿越率 (SC)，$P(Ex \mid SC)$ 表示而当圆柱区域被提出以减少原始立方体的体积时，$R(O)$ 代表通过扩展轨迹面积与表格面积的比率计算出的特定形状的特征 [60]。

4.3. Model improvement

4.3. 模型改进

As discussed in Section 2, the collision probability is calculated separately from each dimension before. This section improves the Event model with 3-D collision probability and the collision radio $R(O)$. Specifically, considering the manoeuvrability (26 options) and accuracy requirements of sUAVs in structured airspace, the modification could help to achieve a better application in the UAV domain.

如第 2 节所述，碰撞概率之前是分别从每个维度计算的。本节通过 3D 碰撞概率和碰撞半径 $R(O)$ 改进事件模型。具体来说，考虑到 sUAV 在结构化空域中的机动性 (26 个选项) 和精度要求，这种修改有助于在无人机领域实现更好的应用。

4.3.1. Collision probability based on the trajectory deviation

4.3.1. 基于轨迹偏差的碰撞概率

In traditional aviation, the standards of trajectory deviation can be required by different navigation performance, e.g., Regional Area Navigation (RNAV) stressed in ICAO 9689 [28]. Since the infrastructure construction of sUAVs is not mature, the sources of TSE is divided into three aspects, path definition, navigation performance and flight error [56]. These factors are integrated to influence. Therefore, most of the research approximates the UAV trajectory deviation to a probability distribution [32,33,53,56]. In the paper, the TSE is expressed as a 3-D Gaussian distribution function.

在传统航空中，轨迹偏差的标准可以根据不同的导航性能要求，例如，国际民航组织 (ICAO)9689 文件中强调的区域导航 (RNAV)[28]。由于小型无人机 (sUAV) 的基础设施建设尚未成熟，轨迹偏差源 (TSE) 被分为三个方面: 路径定义、导航性能和飞行误差 [56]。这些因素综合影响。因此，大部分研究将无人机轨迹偏差近似为概率分布 [32,33,53,56]。在本文中，TSE 被表示为三维高斯分布函数。

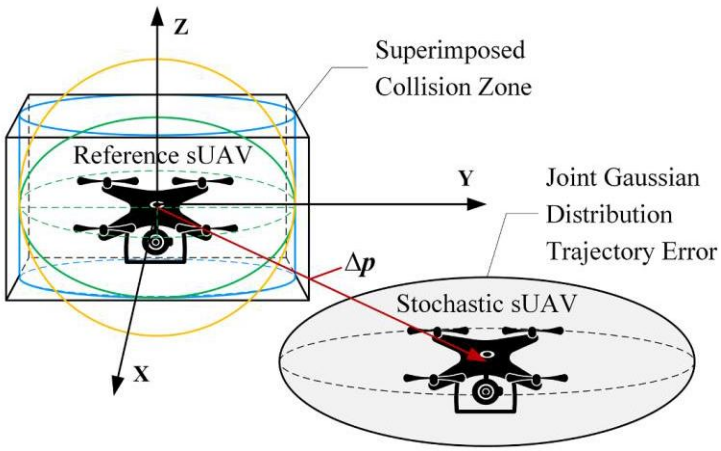

Fig. 7. The calculation of 3-D collision probability.

图 7. 三维碰撞概率的计算。

When obeying the Gaussian distribution, the first approximation of $F_{\text{lon}}(LoWC)$ can be computed as

当符合高斯分布时，$F_{\text{lon}}(LoWC)$ 的一阶近似可以计算为

$$F_{\text{lon}}(LoWC) \cong \delta_{\text{lon}} \cdot P_x(LoWC) \tag{9}$$

Where the δ_{lon} denotes the rate of the separation loss. It is always considered as a statistical correction which reflects system stability and the air traffic density. Therefore, $F(SC)$ can be expressed as

其中 δ_{lon} 表示分离损失率。它通常被视为一个反映系统稳定性和空中交通密度的统计修正。因此，$F(SC)$ 可以表示为

$$F(SC) = \delta_{\text{lon}} \cdot P_{\text{lon}}(LoWC) \cdot P_{\text{lon}}(MAC \mid LoWC) = \delta_{\text{lon}} \cdot P_{\text{lon}}(MAC) \tag{10}$$

Combined with Eq. (8), the product of triple collision probabilities can be improved by 3-D Gaussian distribution integral. Assuming relative position and velocities involved in track deviation are established on the body coordinate system of the sUAV. And, the position coordinates of the sUAV are established on the global coordinate system.

结合方程 (8)，通过三维高斯分布积分，可以改进三重碰撞概率的乘积。假设轨迹偏差中涉及的相对位置和速度建立在 sUAV 的机体坐标系上。并且，sUAV 的位置坐标建立在全局坐标系上。

Let $\overline{\mathbf{p}}(t)$ denotes the nominal position of the sUAV in global coordinate system, and $\widetilde{\mathbf{p}}(t)$ denotes the deviation in body coordinate system. The trajectory deviation can be expressed as

令 $\overline{\mathbf{p}}(t)$ 表示 sUAV 在全局坐标系中的标称位置，$\widetilde{\mathbf{p}}(t)$ 表示机体坐标系中的偏差。轨迹偏差可以表示为

$$\begin{aligned}\mathbf{M}(\psi,\theta) &= \begin{bmatrix}\cos\psi & -\sin\psi & 0\\ \sin\psi & \cos\psi & 0\\ 0 & 0 & 1\end{bmatrix}\begin{bmatrix}\cos\theta & 0 & -\sin\theta\\ 0 & 1 & 0\\ \sin\theta & 0 & \cos\theta\end{bmatrix}\\ &= \begin{bmatrix}\cos\psi\cos\theta & -\sin\psi & -\cos\psi\sin\theta\\ \sin\psi\cos\theta & \cos\psi & -\sin\psi\sin\theta\\ \sin\theta & 0 & \cos\theta\end{bmatrix}\end{aligned} \tag{12}$$

Where ψ denotes the heading angle, and the θ denotes the pitching angle. The position of the UAV in the global coordinate system can be given as $\mathbf{p}(t) = \mathbf{M}\widetilde{\mathbf{p}}(t) + \overline{\mathbf{p}}(t)$. From the properties of the variance transformation, the actual position of the UAV is described as a 3-D Gaussian distribution

其中 ψ 表示航向角，θ 表示俯仰角。无人机在全局坐标系中的位置可以表示为 $\mathbf{p}(t) = \mathbf{M}\widetilde{\mathbf{p}}(t) + \overline{\mathbf{p}}(t)$ 。根据方差变换的性质，无人机的实际位置被描述为三维高斯分布。

$$\mathbf{p}(t) \sim \mathbf{N}_3\left(\overline{\mathbf{p}}(t), \mathbf{M}\Lambda(t)\mathbf{M}^T\right) \tag{13}$$

Base on the assumption of Section 3.2 and 4.1, the joint covariance is assigned to the 'Stochastic UAV', and the 'Reference UAV' can be regarded as no uncertainty of position with the superposed collision zone, as shown in Fig. 7.

基于第 3.2 节和 4.1 节的假设，联合协方差被分配给“随机无人机”，而“参考无人机”可以被视为在叠加碰撞区中位置无不确定性。

The 'Reference sUAV' and the 'Stochastic sUAV' are represented by the subscripts R and S . Obviously, the relative position also obey 3-D Gaussian distribution, which can be expressed as

“参考小型无人机”和“随机小型无人机”分别用下标 R 和 S 表示。显然，相对位置也遵循 3-D 高斯分布，可以表示为

$$\Delta\mathbf{p}(t) = \mathbf{p}_S(t) - \mathbf{p}_R(t) = \mathbf{M}_S\widetilde{\mathbf{p}}_S(t) - \mathbf{M}_R\widetilde{\mathbf{p}}_R(t) + \overline{\mathbf{p}}_S(t) - \overline{\mathbf{p}}_R(t) \tag{14}$$

with the terms set below

使用以下设置的术语

$$\begin{cases}\overline{\mathbf{p}}_S(t) - \overline{\mathbf{p}}_R(t) = \Delta\overline{\mathbf{p}}(t)\\ \mathbf{M}_S\widetilde{\mathbf{p}}_S(t) - \mathbf{M}_R\widetilde{\mathbf{p}}_R(t) = \Delta\widetilde{\mathbf{p}}(t)\\ \mathbf{C} = \operatorname{cov}\left(\Delta\widetilde{\mathbf{p}}(t)\right) = \mathbf{M}_S\Lambda_S(t)\mathbf{M}_S^T + \mathbf{M}_R\Lambda_R(t)\mathbf{M}_R^T\end{cases} \tag{15}$$

then, we obtain that:

然后，我们得到:

$$\Delta\mathbf{p}(t) \sim \mathbf{N}_3\left(\Delta\overline{\mathbf{p}}(t), \mathbf{M}_S\Lambda_S(t)\mathbf{M}_S^T + \mathbf{M}_R\Lambda_R(t)\mathbf{M}_R^T\right) \tag{16}$$

Besides, to express the superposed collision zone (integration region), the primary position of 'Reference sUAV' is set as

此外，为了表示叠加碰撞区 (积分区域)，将“参考小型无人机”的主要位置设置为

$$\mathbf{p}_{R0} = \begin{bmatrix} x_0 & y_0 & z_0 \end{bmatrix}^T \tag{17}$$

$$\mathbf{p}_R = \begin{bmatrix} x - x_0 & y - y_0 & z - z_0 \end{bmatrix}^T = \begin{bmatrix} r_2 & r_3 & r_1 \end{bmatrix}^T \tag{18}$$

If D denotes the superimposed collision zone $D_{Cu}, D_{Sp}, D_{Cy}, D_{El}$ and D_{Com} denote the cuboid, Sphere, cylinder, Ellipsoid, and Combined zone respectively, then

如果 D 表示叠加碰撞区 $D_{Cu}, D_{Sp}, D_{Cy}, D_{El}$，而 D_{Com} 分别表示长方体、球体、圆柱体、椭球体和组合区域，那么

$$D = \begin{cases} \\ \left\{ \mathbf{p}_R \in \mathbb{R}^3 : [r_2, r_3]^2, r_2 \le (R_S + R_R)^2, (R_S + R_R)^2, (R_S + R_R)^2, (R_S + R_R)^2, (R_S + R_R)^2, (R_S + R \right. \end{cases} \tag{19}$$

$$\widetilde{\mathbf{p}}(t) \sim \mathrm{N}(0, \Lambda(t)) \tag{11}$$

where $\square(t) = \mathrm{diag}\left(\sigma_x^2(t), \sigma_y^2(t), \sigma_z^2(t)\right)$ represents the directional variance. And $\sigma_i^2(t)$ is the variance of the deviation along the coordinate axis. Therefore, the transformation matrix from the body coordination to the global coordinate system can be expressed as.

其中 $\square(t) = \mathrm{diag}\left(\sigma_x^2(t), \sigma_y^2(t), \sigma_z^2(t)\right)$ 表示方向方差。而 $\sigma_i^2(t)$ 是沿坐标轴偏差的方差。因此，从机体坐标系到全局坐标系的转换矩阵可以表示为。

Thus, the collision probability between two sUAV during a period Tcould be computed as

因此，在时间周期 T 内两小型无人机之间的碰撞概率可以计算为

$$P(MAC) = P(kT_s)$$

$$= \iiint_{\Delta\mathbf{p}(kT_s) \in D} \mathbf{N}_3\left(\Delta\mathbf{p}(kT_s); \Delta\overline{\mathbf{p}}(kT_s), \mathbf{M}_S \Lambda_S(kT_s) \mathbf{M}_S^T + \mathbf{M}_R \Lambda_R(kT_s) \mathbf{M}_R^T\right) d\Delta\mathbf{p} \tag{20}$$

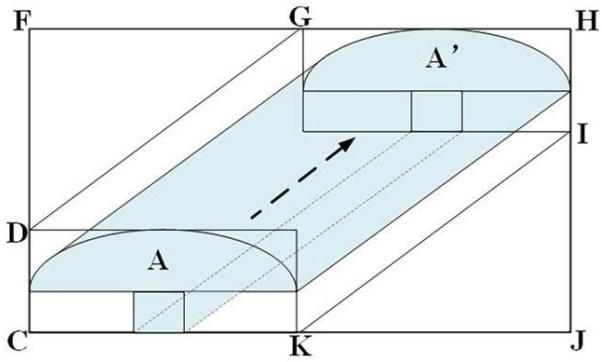

Fig. 8. The improved extended collision zone.

图 8. 改进的扩展碰撞区。

Table 1

表 1

Relationship between the directional separations and encountering scenarios

方向分离与遭遇场景之间的关系 [28].

Separations	Encountering Scenarios	Utilization	Safety Threshold
Longitudinal	Single Route	Radius of Self-	TLS
Separation	Crossing Routes	Separation	(Rate of
Lateral	Parallel Routes with	Width of Air	collision)
Separation	Same Altitude	Route centerline	
Vertical	Parallel Routes with	Flight Levels and	
Separation	Different Altitudes	Altitudes	

分离过程	遭遇场景	利用	安全阈值
纵向	单一路径	自身半径	TLS
分离	交叉航线	分离	(速率 of
横向	与之平行的航线	空域宽度	碰撞)
分离	同一高度	航线中心线	
垂直	与之平行的航线	飞行高度和	
分离	不同高度	高度	

where $k \in M, M = \{i \in \mathbb{N} : i \leq \lfloor T/T_s \rfloor, 0 < T_s \leq T\}, T_s$ denotes the sampling period.
其中 $k \in M, M = \{i \in \mathbb{N} : i \leq \lfloor T/T_s \rfloor, 0 < T_s \leq T\}, T_s$ 表示采样周期。

4.3.2. Collision ratio

4.3.2. 碰撞比例

$R(O)$ is the ratio of the trajectory area left on the sheet from the dynamic movement of collisions, representing the comparison of different shapes [60]. However, the cruising speed of the traditional civil aircraft is great compared with the fuselage scale, resulting that needs little time to cross the 'sheet'. Furthermore, the area of the rectangular 'C-F-H-J' is easy to calculate as an approximation term instead of the hexagon 'C-D-G-H-I-K', that also reflects the 'conservative risk assessment' to over-estimate risk [50].

$R(O)$ 是由动态碰撞运动在板材上留下的轨迹区域的比例，代表不同形状的比较 [60]。然而，与传统民用飞机的机身尺度相比，其巡航速度较大，导致穿过' 板材' 的时间很短。此外，矩形'C-F-H-J' 区域的面积易于计算，作为近似项代替六边形'C-D-G-H-I-K'，这也反映了' 保守风险评估' 以高估风险 [50]。

In this paper, the collision ratio is defined as the ratio of the area of the track crossed by the superimposed collision zone to the area of the hexagon. Due to rotor-wing fuselage, collision attitude changes and other dynamic effects. we adopt the maximum cross-section for derivation which is also recognized as a simplification, depicted in Fig. 8. The basic area of hexagon is computed as

在本文中，碰撞比例定义为叠加碰撞区穿过的轨迹面积与六边形面积之比。由于旋翼-机身、碰撞姿态变化等动态效应，我们采用最大横截面进行推导，这在图 8 中也被视为一种简化。六边形的基本面积计算为

$$S_1 = 8R_f \left[H_f + 2R_f \frac{v'_z}{v'_x} + H_f \frac{v'_y}{v'_x} \right] \tag{21}$$

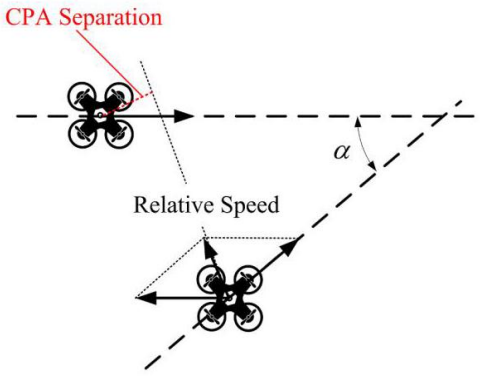

Fig. 9. CPA separation.
图 9. CPA 分离。

Where the R_f, H_f are the parameters of the superimposed collision zone. $v'_i(x, y, z)$ are velocities relative to the sheet plane. Let S_2 denotes the maximum cross-sectional expression for each shape.
其中 R_f, H_f 是叠加碰撞区的参数。$v'_i(x, y, z)$ 是相对于板材平面的速度。让 S_2 表示每个形状的最大横截面表达式。

$$S_2 = \begin{cases} 8R_f\left(H_f + 2R_f^{\frac{V_2}{V_x}} + H\frac{V_y}{V_x}\right) & D = D_{\text{Cubioid}}\, D_{\text{Cylinder}} \\ 4R_f^2\left(\pi + 4\sqrt{v_y^{V_x} + v_z'^2}\right) & D = D_{\text{Sphere}} \\ 2\pi R_f H_f + 8R\frac{V_y}{V_x^2}\sqrt{H_f^2 + 4R_f^2\left(\frac{V_z}{V_y}\right)^2} & D = D_{\text{Ellipsoid}} \\ 8R_f\frac{V_x}{V_x} + \pi R_f H_f + 4ac + 2\frac{V_x^2}{V_x^2}a^2 & D = D_{\text{ConiniotalCone}} \\ 4R_f a^2\sqrt{H_f^2 + 4R_f^2\left(\frac{V_x}{V_y}\right)^2} & D = D_{\text{ConinoidConce}} \end{cases} \tag{22}$$

Therefore, the collision ratio can be obtained by
因此，可以通过以下方式获得碰撞比例

$$R(O) = S_2/S_1 \tag{23}$$

Consequently, the collision risk model for sUAVs is established by the improvements. For an instance, the longitudinal collision risk can be computed as
因此，通过改进建立了用于小型无人机的碰撞风险模型。例如，纵向碰撞风险可以计算为

$$F_{\text{lon}}\ (kT_s) = 2R(O)\cdot\delta_{\text{lon}}\cdot P(MAC)\cdot\left(1+\frac{2v_z'R_f}{v_x'H_f/2}\right)\left(1+\frac{v_y'R_f}{v_x'R_f}\right) \tag{24}$$

When there are N pairs of sUAVs in the operational system, the collision risk of the system could be calculated as
当操作系统中存在 N 对小型无人机时，系统的碰撞风险可以计算为

$$CR = \sum_i F_n^i\,(kT_s) \tag{25}$$

The rate of the separation is the statistical value by trials [60], since there is rare research or trials on the specific level for δ_n in UTM. In the paper, we set the $\delta_{\text{lon}} = 10^{-2}$, and $\delta_{\text{ver}} = \delta_{\text{lat}} = 10^{-3}$, which is the same as traditional aviation [61].
分离率是通过试验得到的统计值 [60]，因为在通用空中交通管理 (UTM) 中很少有关于 δ_n 的具体级别的研究或试验。在本文中，我们设定了 $\delta_{\text{lon}} = 10^{-2}$ 和 $\delta_{\text{ver}} = \delta_{\text{lat}} = 10^{-3}$，这与传统航空相同 [61]。

4.4. Demarcation of safe separations

4.4. 安全间隔的划分

The separations demarcated in the paper is corresponding to the well clear volume and air route design. This section illustrates the relations between the separations and the applicational scenarios. Besides, the conservative principle of risk estimation is also elaborated.
论文中划分的间隔对应于清晰体积和航线设计。本节说明了间隔与应用场景之间的关系。此外，还详细阐述了风险评估的保守原则。

4.4.1. Classification of separations

4.4.1. 间隔的分类

In traditional aviation, the separations can be divided by the measurement, e.g., time-based separations and distance-based separations. While the applications of position equipment makes the latter one is more effective [15]., e.g., Automatic Dependance Surveillance-Broadcasting (ADS-B) and Global Navigation Satellite System (GNSS), the time-based separations refer to the procedure control and the avoidance of vortex [28]. Based on the TLS and the intersection model recommended by ICAO 9689, the distance-based separations and the encountering scenarios are summarized in Table 1.
在传统航空中，间隔可以根据测量进行划分，例如基于时间的间隔和基于距离的间隔。而位置设备的应用使得后者更加有效 [15]，例如自动依赖监视广播 (ADS-B) 和全球导航卫星系统 (GNSS)，基于时间的

间隔指的是程序控制和涡流的避免 [28]。基于 ICAO 9689 推荐的 TLS 和交叉模型，基于距离的间隔和遭遇场景在表 1 中进行了总结。

Hence, with the predesigned safety target (ELoS), separations for tube-type routed can be demarcated by corresponding encountering scenarios for sUAVs, as longitudinal separations by spacing aircraft with a specified distance, width and height of air routes centerline for lateral and vertical case. Note that the longitudinal separation is also taken for the crossing routes. Then, the separations in the horizontal plane are considered as the radius of the self-separation volume. In addition to improve operational efficiency and capacity, it is necessary to reveal the mechanics of collision risk changing with angle.

因此，有了预设的安全目标 (ELoS)，对于管道型路由的间隔可以通过相应的遭遇场景来划分，对于 sUAVs，纵向间隔是通过指定距离、航线中心线的宽度和高度来间隔飞机，横向和垂直情况也是如此。注意，交叉路线也采用纵向间隔。然后，水平平面上的间隔被视为自我间隔体积的半径。为了提高运营效率和容量，有必要揭示碰撞风险随角度变化机理。

Table 2
表 2
Parameters of DJ Matrice 600 Pro.
DJ Matrice 600 Pro 的参数。

Parameter	Value
Size	$1668 \times 1518 \times 727$ mm
Maximum Speed	Horizontal: 18 m/s Ascent: 5 m/s , Descent: 3 m/s
Positioning Accuracy	Horizontal: ± 0.5 m , Vertical: ± 1.5 m

参数	值
尺寸	$1668 \times 1518 \times 727$ mm
最大速度	水平: 18 m/s 上升: 5 m/s ， 下降: 3 m/s
定位精度	水平: ± 0.5 m ， 垂直: ± 1.5 m

Table 3
表 3
Parameters of simulation environment.
仿真环境的参数。

Numbers	Wingspan (m)	Height (m)	Separations of each pair (m) $\Delta \mathbf{p}\,(x, y, z)$	Relative speed of each pair (m/s) $v_i'\,(x, y, z)$
200	U(0, 10)	U $(0, 3)$	U $(0, 30)$, N $(0, 1)$, N (0,1)	N $(6, 1)$, N $(0, 1)$, N (0,1)

数量	翼展 (米)	高度 (米)	每对之间的分离距离 (m) $\Delta \mathbf{p}\,(x, y, z)$	每对的相对速度 (m/s) $v_i'\,(x, y, z)$
200	U(0, 10)	U $(0, 3)$	U $(0, 30)$, N $(0, 1)$, N (0,1)	N $(6, 1)$, N $(0, 1)$, N (0,1)

According to the assumption in Section 4.1, the relative movement between sUAVs can be obtained with constant speed and directions set preliminarily. So, there is a Closest Point of Approach (CPA) [33], as shown in Fig. 9. The paper demarcates the relative distances until CPA in crossing scenarios, to refine the criteria of separations for sUAV. Additionally, since the crossing routes with different angles will have the specific safety separation, the maximum of them is adopted.

根据第 4.1 节的假设，sUAVs 之间的相对运动可以通过预设的恒定速度和方向获得。因此，存在一个最近接近点 (CPA)[33]，如图 9 所示。本文划分了在交叉场景中直到 CPA 的相对距离，以优化 sUAV 的分离标准。另外，由于不同角度的交叉路线将有特定的安全间隔，因此采用其中的最大值。

4.4.2. Conservative principle of risk estimation

4.4.2. 风险估计的保守原则

Differ from the collision detection and resolution, the demarcation of separations is mostly based on the unmitigated collision risk [13,19]. The unmitigated conditions assert that the collision risk is independent of human intervention, DAA, or any other separation maneuver. In other words, the desired unmitigated risk threshold is achieved, if the well clear separations are maintained by sUAVs. Meanwhile, the set of encountering scenarios seems to be 'extreme'. For an instance, to reveal the correlation between collision risk and separations, we set the encountering scenarios in that the sUAVs fly with one-dimensional separation tend to zero. Generally, the safety and reliability

of the separation are considered primarily with conservative estimation of risk [50], so that the criteria could satisfy the safety level in any other states of operations.

与碰撞检测和解决不同，分离的划分主要基于未减轻的碰撞风险 [13,19]。未减轻的条件假定碰撞风险独立于人为干预、DAA 或任何其他分离操作。换句话说，如果 sUAVs 保持清晰的安全间隔，则可以实现期望的未减轻风险阈值。同时，遇到的场景似乎趋于“极端”。例如，为了揭示碰撞风险与分离之间的相关性，我们设定了 sUAVs 以一维分离趋近于零的遭遇场景。通常，安全间隔的安全性和可靠性主要考虑风险的保守估计 [50]，以便标准能够满足任何其他操作状态下的安全水平。

As illustrated in Section 3, the redefined collision zone is established to be extreme case for sNMAC, the safety thresholds for well clear in the paper are based on the conditional rate or probability of MAC determined by the collision zone. It is a trade-off between collision determination and unsuitable adoption from previous definition. And we assume that the collision zone provides the baseline for sNMAC in the future, where the safety is assured by diversified separations in structured airspace. Consequently, the ’ ELoS $= 10^{-7}$MAC per flight hour’ is utilized as an unambiguous criterion of separations in the paper, that is the generalized by statistics of National Transportation Safety Board (NTSB) [25].

如第 3 节所示，重新定义的碰撞区域被建立为 sNMAC 的极端情况，文中关于“清晰间隔”的安全阈值是基于由碰撞区域确定的 MAC 的条件速率或概率。这是在碰撞判定与从前定义的不适用采纳之间的权衡。我们假设碰撞区域为未来 sNMAC 提供了基准，在该基准中，通过结构化空域中的多样化间隔来确保安全。因此，在文中，“每飞行小时的 ELoS $= 10^{-7}$MAC ”被用作间隔的明确标准，即由美国国家运输安全委员会 (NTSB)[25] 的统计数据推广而来。

Additionally, RTCA SC-228 adopted well clear of 2.2 % collision probability with the modification from 5% [34]. P (NMAC ｜ LoWC) $=$ 5% is recommended by relevant researches as candidate in the primary stage [37, 38, 41] , where safety evaluation is conducted in the open-loop [41]. While there is also no consensus on well clear definition of sUAVs-only encounters, let alone operations in structured airspace, the $P\,(sNMAC \mid LoWC) =$ 5% (omitted as ’ 5 % sNMAC’ below) is selected to conduct the preliminary comparative analysis of ’ELoS’.

此外,RTCA SC-228 采用了修改后的 5% 2.2% 的碰撞概率来定义“清晰间隔”[34]。P (NMAC ｜ LoWC) $=$ 5% 的相关研究推荐作为初步阶段的候选者 [37, 38, 41] ，在此阶段进行了开环的安全评估 [41]。虽然在仅 sUAVs 遭遇的“清晰间隔”定义上还没有共识,更不用说在结构化空域中的操作,但 $P\,(sNMAC \mid LoWC) =$ 5% (以下省略为“5%sNMAC”) 被选用来进行“ELoS”的初步比较分析。

5. Numerical simulation

5. 数值模拟

All numerical simulation tests in this paper are carried out in MAT-LAB 2019 a. The computer processor is Intel(R) Core (TM) i7-8750 H CPU @2.20GHZ and the random-access memory (RAM) was 8 GB. The MATLAB Interal3 function is used as the exact solution of the three-dimensional Gaussian distribution integral. DJ Matrice 600 Pro was selected as the experimental object, equipped with GNSS transceiver. Parameters are summarized in Table 2.

本文的所有数值模拟测试均在 MATLAB 2019 a 中进行。计算机处理器为 Intel(R) Core(TM) i7-8750 H CPU @2.20GHZ，随机存取存储器 (RAM) 为 8 GB。MATLAB Interal3 函数被用作三维高斯分布积分的精确解。选择 DJ Matrice 600 Pro 作为实验对象，配备了 GNSS 收发器。参数在表 2 中总结。

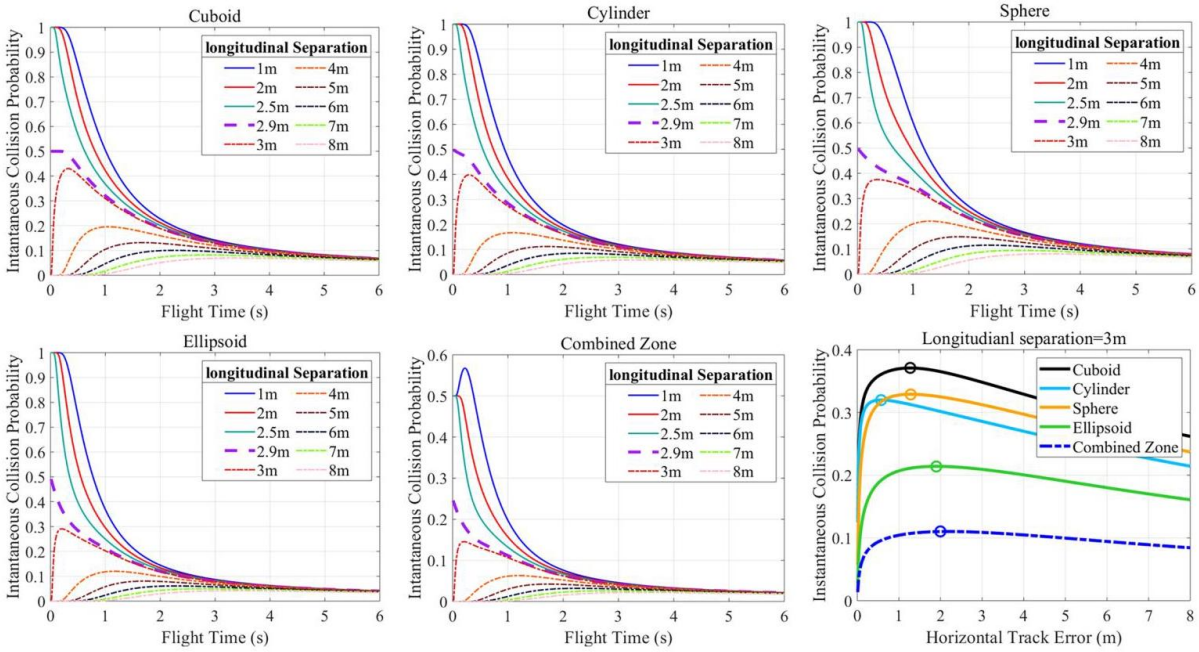

Fig. 10. Sensitivity analysis of longitudinal track deviation.
图 10. 纵向轨迹偏差的敏感性分析。

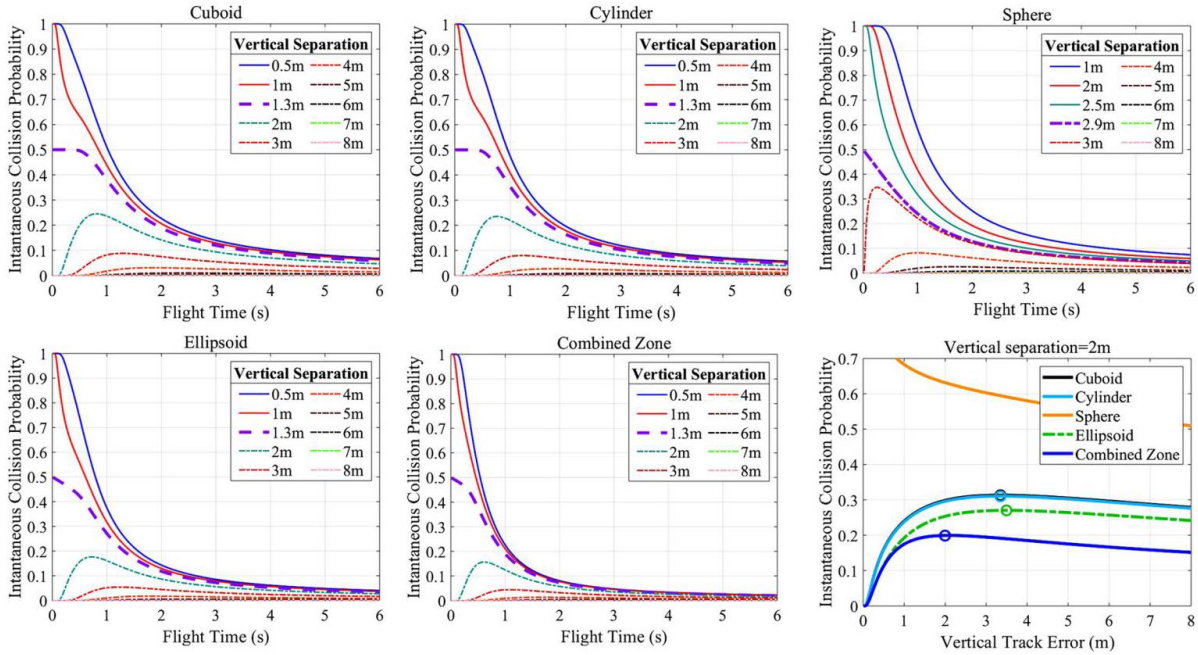

Fig. 11. Sensitivity analysis of vertical track deviation.
图 11. 垂直轨迹偏差的敏感性分析。

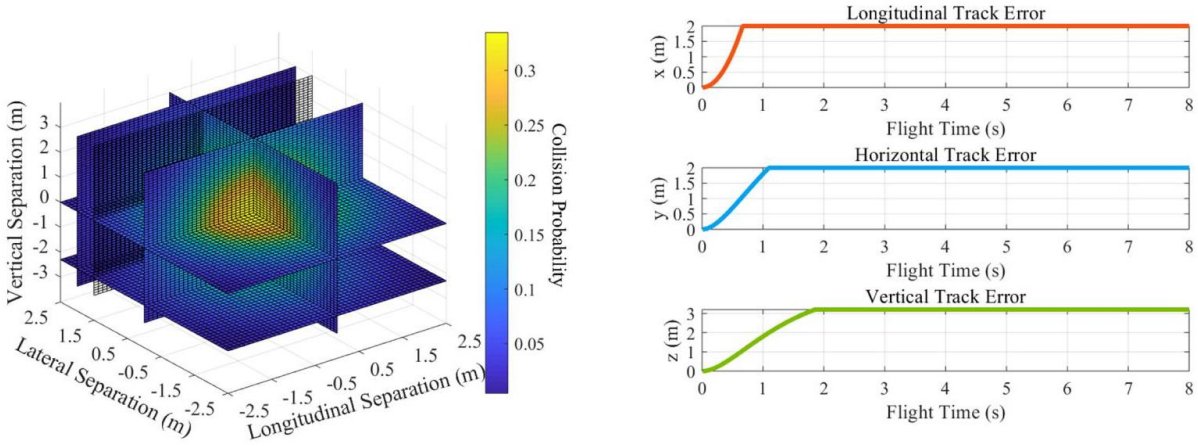

(**a**) Cylindrical zone

(**b**) The change of track deviation.

Fig. 12. 3-D probability density.

图 12. 3-D 概率密度。

According to Eq. (1), the size of the collision zone after the superposition of the two DJ Matric 600 Pro is computed as $R_D = 2 \cdot \sqrt{3} r_D$, rounded up to 2.9 m, $H_D = 2 \cdot \sqrt{3} h_D$, rounded up to 2.6 m . Then, trajectory error covariance sUAV is computed as [33]

根据 (1) 式，两个 DJ Matric 600 Pro 叠加后的碰撞区域大小计算为 $R_D = 2 \cdot \sqrt{3} r_D$ ，向上取整为 2.9 m, $H_D = 2 \cdot \sqrt{3} h_D$ ，再向上取整为 2.6 m 。然后，无人机轨迹误差协方差 sUAV 计算为 [33]。

$$\square(t) = \begin{cases} \sigma_x(t) = t\left(p_a \cos\theta(t) + p_b \sin\theta(t)\right) \\ \sigma_y(t) = p_a\left(1 - \exp\left(-t/t_a\right)\right) \\ \sigma_z(t) = \left(p_a \cos\theta(t) + p_b \sin\theta(t)\right)\left(1 - \exp\left(-t/t_b\right)\right) \end{cases} \tag{26}$$

Where θ is the climbing and descending angle of sUAV, and $p_a = 1.5, p_b = 0.5$ corresponding to the positioning accuracy in Table 2, $t_a = t_b = 1$ s . In addition, the mean ascent, descent and horizontal speeds are assumed as 2 m/s, 3 m/s, 6 m/s . The size of cargo after superimposed is 1.2 m × 1 m× 0.8 m .

其中 θ 是 sUAV 的爬升和下降角度，$p_a = 1.5, p_b = 0.5$ 对应于表 2, $t_a = t_b = 1$ s 中的定位精度。此外，假设平均上升、下降和水平速度分别为 2 m/s, 3 m/s, 6 m/s 。叠加后的货物大小为 1.2 m × 1 m× 0.8 m 。

5.1.TSE based on trajectory deviation

5.1. 基于轨迹偏差的 TSE

As discussed in Section 2.3, and Eq. (20), the TSE is modelled as the 3-D Gaussian distribution function, which has been revealed by real trials [32]. Zou [33]and Kim [62]assumed the trajectory deviation increase over time without a boundary. Obviously, the hypothesis is doubtful for sUAVs when operating with high refresh-rate equipment, even GPS signal is intermittent [31]. It is necessary to set the outer bound of deviation while relevant studied have been carried out to determine the significance level [56]. In the section, to determine the reliable supremum of TSE, we conducted the sensitivity analysis to trajectory deviation for collision probability. Assuming that the increasing rate is 1 m/s , the changes are depicted with separations fixed, shown in Figs. 10 and 11.

如第 2.3 节和 (20) 式所述，TSE 被建模为 3-D 高斯分布函数，这一点已经通过实际试验 [32] 得到验证。Zou [33] 和 Kim [62] 假设轨迹偏差随时间增加而没有边界。显然，当 sUAV 使用高刷新率设备运行时，即使 GPS 信号中断 [31]，这一假设也是值得怀疑的。在相关研究已经确定显著性水平 [56] 的同时，有必要设定偏差的外部边界。在本节中，为了确定 TSE 的可靠最大值，我们对轨迹偏差对碰撞概率的敏感性进行了分析。假设增加率为 1 m/s ，变化情况在固定分离距离下展示，如图 10 和 11 所示。

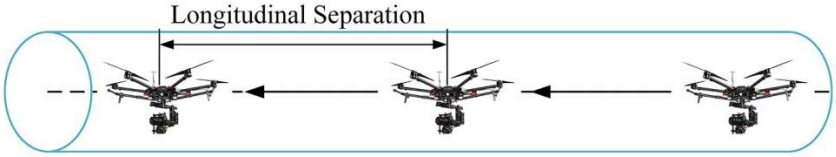

Fig. 13. Single Route.
图 13. 单一路径。

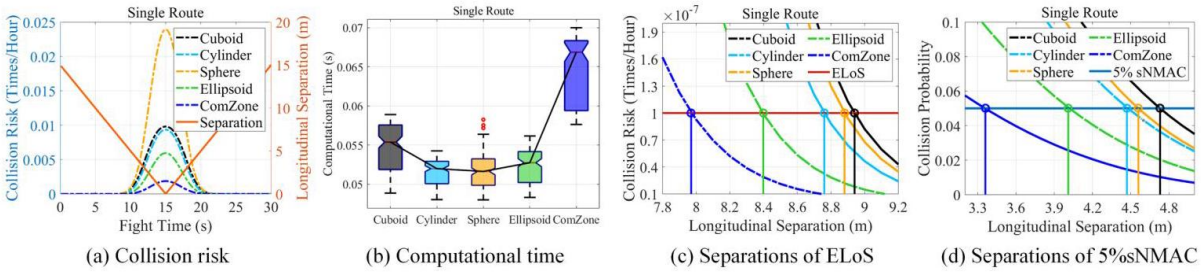

(a) Collision risk (b) Computational time (c) Separations of ELoS (d) Separations of 5%sNMAC

Fig. 14. The demarcation of longitudinal separations.
图 14. 纵向分离界限。

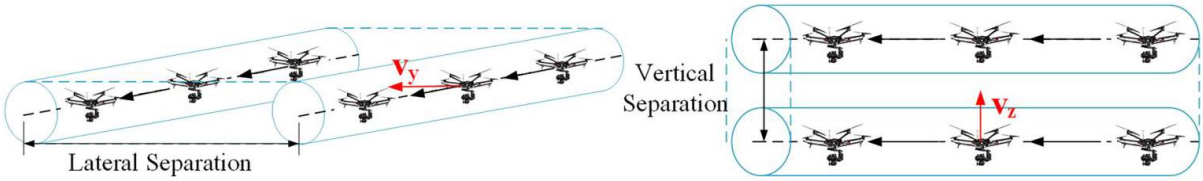

Fig. 15. Parallel Routes.
图 15. 平行路径。

The results indicate the high correlation between trajectory deviation and collision probability, finally convergent to 0.1 . Then, regardless of shapes, there is a gap of changes at the longitudinal separation of 2.9 m and vertical separation of 1.3 m , consistent with judgement in Eq. (3). Meanwhile, if the separation is greater than size scale, there is a peak of probability with the deviation increases. The mechanism provides us a reference that the deviation with peak value could be tractable for the upper boundary of TSE. The separations are selected where the collision is about to happen, 3.0 m horizontally, 2.0 m vertically. Hence, the supremum of trajectory deviation is established by the maximum peaks of each collision zones, 2.0 m horizontally and 3.2 m vertically. Consequently, choosing an appropriate bound will be a balance between simplification and conservativeness.

结果表明轨迹偏差与碰撞概率之间存在高度相关性，最终收敛至 0.1。随后，无论形状如何，在纵向间隔为 2.9 m 和垂直间隔为 1.3 m 处存在一个变化间隙，这与方程 (3) 中的判断一致。同时，如果间隔大于尺度大小，随着偏差的增加，概率会出现峰值。该机制为我们提供了一个参考，偏差的峰值可能是 TSE 上限的可处理值。选择的间隔是在碰撞即将发生的位置，3.0 m 水平方向，2.0 m 垂直方向。因此，轨迹偏差的上确界由每个碰撞区域的最大峰值建立，2.0 m 水平方向和 3.2 m 垂直方向。因此，选择一个合适的边界将是简化与保守之间的平衡。

Hence, the trajectory error covariance is set as $\mathbf{C} = \mathrm{diag}\,(2, 2, 3.2)$. The flight trails provided the convincing evidence that the RNP of the similar sUAV (DJ M600) is determined as 2.91 m , when the confidence interval is 99.999% [58]. Taking the cylindrical zone as an instance, the collision probability diagram of two sUAVs with different relative positions is presented in Fig. 12. Integral result of the 3-D distribution is regarded as an ellipsoid approximately whose shape features are determined byC. Then, the scenarios are classified into three types, single route, parallel routes, and crossing routes, summarized in Table 1. The collision risk is computed to demarcate the separations with the threshold of 'ELoS'. In addition, the paper records the computational time of each calculation of collision zones, as an evaluation indicator.

因此，轨迹误差协方差设置为 $\mathbf{C} = \mathrm{diag}\,(2, 2, 3.2)$ 。飞行试验提供了令人信服的证据，表明类似的小型无人机 (DJ M600) 的 RNP 确定为 2.91 m ，当置信区间为 99.999% [58] 时。以圆柱形区域为例，图 12 展示了两个相对位置不同的小型无人机之间的碰撞概率图。三维分布的积分结果被视为一个近似椭球体，其形状特征由 C 确定。然后，将场景分类为三种类型，单一路径、平行路径和交叉路径，总结在表 1 中。计算碰撞风险以划分与'ELoS' 阈值的间隔。此外，本文记录了每个碰撞区域计算的计算时间，作为评估指标。

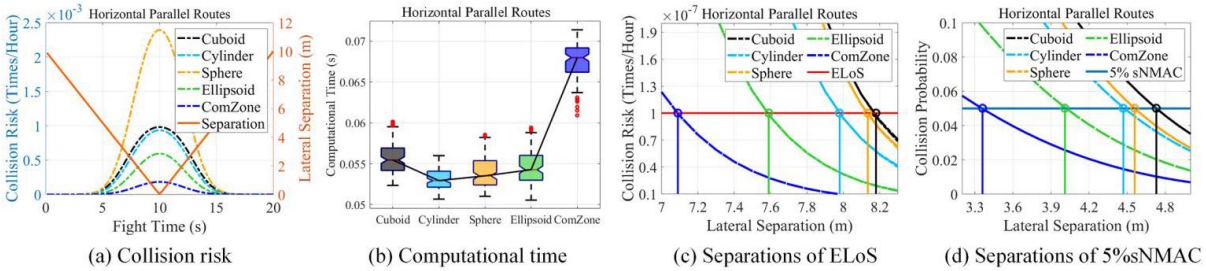

(a) Collision risk (b) Computational time (c) Separations of ELoS (d) Separations of 5%sNMAC

Fig. 16. The demarcation of lateral separations.
图 16。侧向间隔的划分。

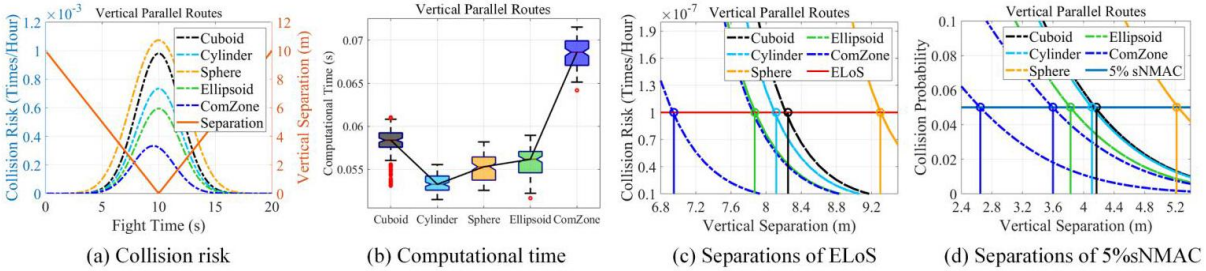

(a) Collision risk (b) Computational time (c) Separations of ELoS (d) Separations of 5%sNMAC

Fig. 17. The demarcation of vertical separations.
图 17。垂直间隔的划分。

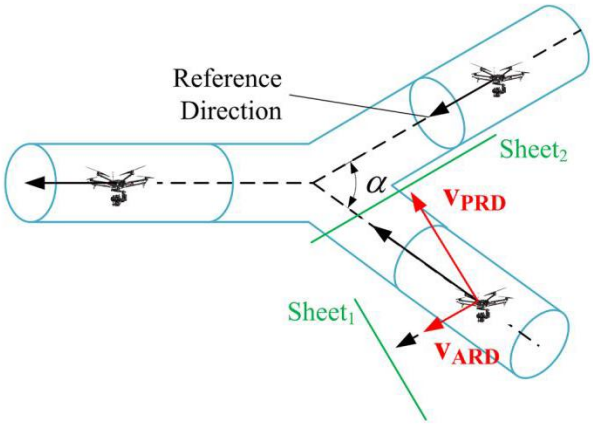

Fig. 18. Crossing Routes.
图 18。交叉路径。

5.2. Single route

5.2. 单一路径

Assuming that there are two sUAVs flying in single route horizontally with separation of 15 m (see Fig. 13), and approaching with 1 m/s , the collision risks along with time for different collision zones are shown in Fig. 14. Fig. 14(a) indicates that the collision risk can be well identified in proportion to separations, regardless of shapes. However, it still presents the dramatic difference between sphere and others, especially with separations reduce to 0 . More collision volume produces the more conservative results in collision risk. The computational time shows the positive correlation with complexity of shape, e.g., combined zone. While it exceeds the expectation that the cuboid has the greater time cost than other smooth shapes. Based on the Fig. 14(a), (b), We believe that

the selection of the appropriate shape helps to achieve the optimal tradeoff between safety margin and efficiency in UTM.

假设有两架小型无人机 (sUAVs) 在水平方向上以 15 m 的间隔沿单一路径飞行 (见图 13)，并以 1 m/s 接近，不同碰撞区域随时间的碰撞风险如图 14 所示。图 14(a) 表明，无论形状如何，碰撞风险可以很好地与间隔成比例地识别出来。然而，它仍然呈现了球体与其他形状之间的显著差异，尤其是当间隔减少到 0 时。更大的碰撞体积导致碰撞风险的计算结果更加保守。计算时间与形状的复杂度呈正相关，例如，组合区域。而令人意外的是，立方体的时间成本比其他光滑形状更高。基于图 14(a) 和 (b)，我们认为选择合适的形状有助于在无人机交通管理 (UTM) 中实现安全边际和效率之间的最佳平衡。

According to Eq. (20) and Eq. (24), the separations are demarcated by the threshold of ’ ELoS’ and ’ 5 % sNMAC’ , depicted in Fig. 14(c) and (d). Align with the collision risk, the minimum separations perform high correlation with volume of collision zones. Besides, due to the redefined collision zones and the supremum of trajectory deviation, the safety separations of ’5 % sNMAC’ provide less space than ’ELoS’ for conflict resolution. It indicates that the 5% sNMAC is not suitable to maintain well clear for operations in structured airspace, which may fail to meet the target safety level. Although separations by ’5 % sNMAC’ could be adjusted by down selecting the threshold, e.g., 2.2%, 1% , the collision probability is a metric which faces to safety of each two objects instead of the airspace. In other words, the ’5 % sNMAC’ could be utilized as the collision boundary for DAA in structured airspace when the ’ELoS’ is failed to be maintained.

根据 (20) 式和 (24) 式，分离由’ELoS’ 和’5 % sNMAC’ 的阈值划分，如图 14(c) 和 (d) 所示。与碰撞风险对齐，最小分离距离与碰撞区域的体积表现出高度相关性。此外，由于重新定义的碰撞区域和轨迹偏差的最大值，’5 % sNMAC’ 的安全分离距离为冲突解决提供的空间小于’ELoS’。这表明在结构化空域中，5% sNMAC 不足以保持清晰的安全间隔，可能无法满足目标安全水平。尽管可以通过降低阈值来调整’5 % sNMAC’ 的分离距离，例如 2.2%, 1% ，但碰撞概率是一种面向两个对象安全的度量，而不是空域。换句话说，当无法保持’ELoS’ 时，’5 % sNMAC’ 可用作结构化空域中 DAA 的碰撞边界。

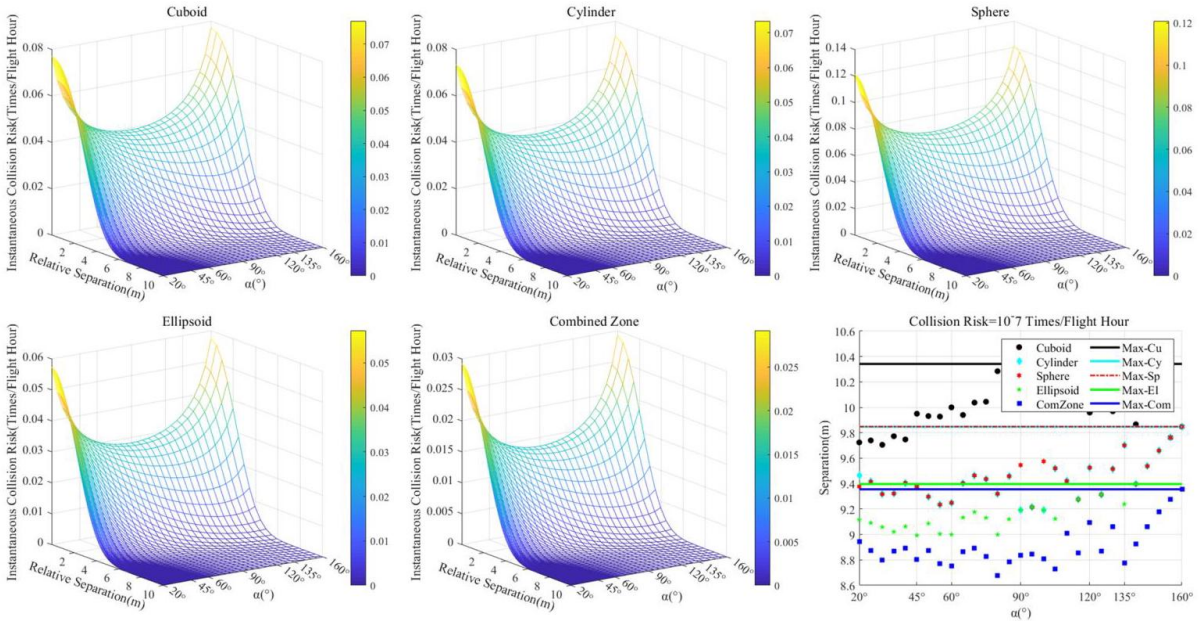

Fig. 19. The demarcation of relative separations in horizontal convergence routes.
图 19. 水平汇聚航线上相对分离距离的划分。

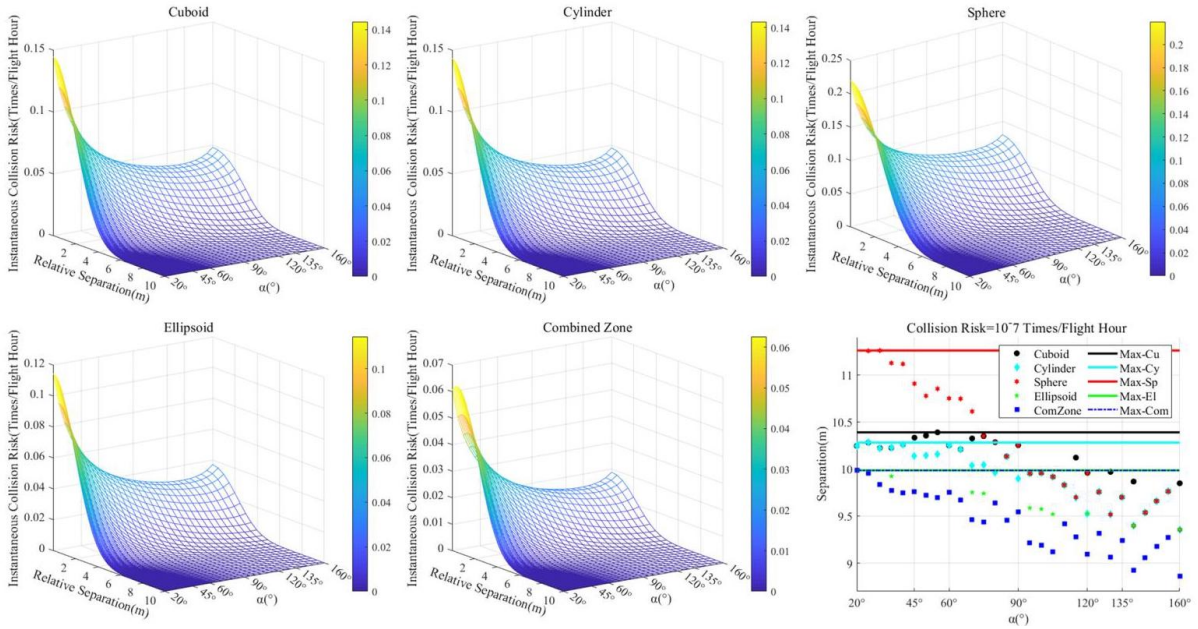

Fig. 20. The demarcation of relative separations in vertical convergence routes.
图 20. 垂直汇聚航线上相对分离距离的划分。

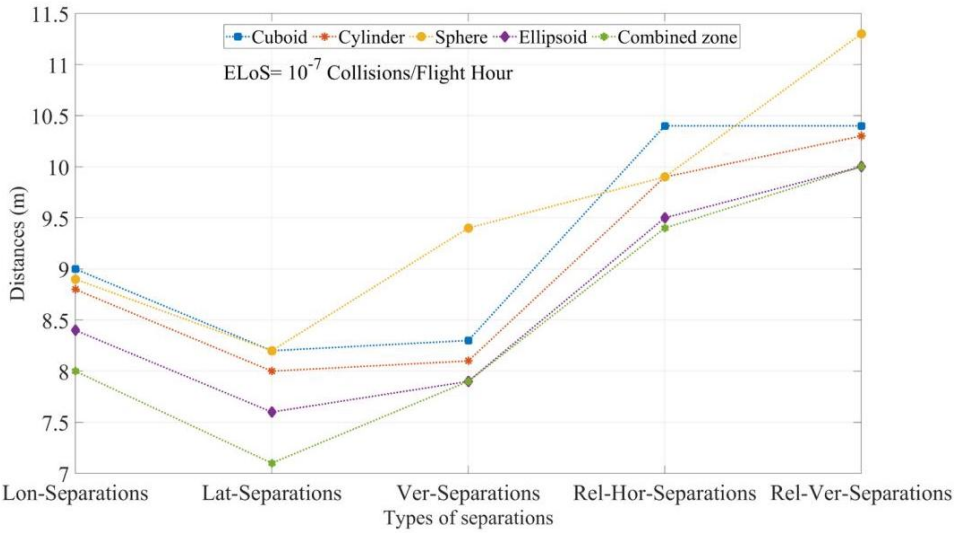

Fig. 21. Separations between two sUAVs based on 'ELoS'.
图 21. 基于'ELoS' 的两架 sUAV 之间的分离距离。

5.3. Parallel routes

5.3. 平行航线

The parallel route scenario means that the two routes have a certain lateral or vertical separation, corresponding to the air routes design summarized in Table 1. In the section, the routes with parallel tracks are utilized to determine the minimum lateral and vertical separations between two sUAVs. We assume that two sUAVs only have a primary separation of 10 m , approaching with 1 m/s , depicted in Fig. 15.

平行航线场景意味着两条航线有一定的横向或垂直间隔，对应于表 1 中总结的航线设计。在本节中，使用平行航迹的航线来确定两架 sUAV 之间的最小横向和垂直间隔。我们假设两架 sUAV 只有一个主要间隔为 10 m ， 以 1 m/s 接近，如图 15 所示。

The results of are roughly similar to the former, shown in Figs. 16 and 17. Considering of the safety and computational time, the cylinder and ellipsoid have the obvious advantages. Also, 'ELoS' is more reasonable to maintain well clear in structured airspace, compared with the 5% sNMAC.

结果大致类似于前者，如图 16 和 17 所示。考虑到安全性和计算时间，圆柱体和椭球体具有明显的优势。此外，与 5% sNMAC 相比，'ELoS' 在保持结构化空域的清晰性方面更为合理。

Due to the asymmetrical characteristics of combined zone in the vertical dimension, the peak of collision risk shifts from the original space that is also reflected on the separations demarcated in Fig. 17. Thus, the different separations could be conducted when the sUAVs have an unsmooth shape, e.g., cargo carrying, inspection. Also, the peak gap is narrowed in collision risk between sphere and others, compared with longitudinal and lateral dimensions above. However, owing to its vertical size scale, sphere should have a larger separation boundary than cuboid (about 1.1 m) which is also different than before. Additionally, the cylinder shows greater performance than before in computational time.

由于垂直维度上结合区域的不对称特性，碰撞风险的高峰值从原始空间转移，这也反映在图 17 中的分离界限上。因此，当 sUAVs 具有不规则的形状，例如，载货或检查时，可以采用不同的分离距离。与上述纵向和横向维度相比，球体与其他形状之间的碰撞风险峰值差距缩小。然而，由于球体的垂直尺寸，球体应该具有比长方体更大的分离边界 (约为 1.1 m)，这与之前不同。此外，圆柱体在计算时间上的性能比之前有更大的提升。

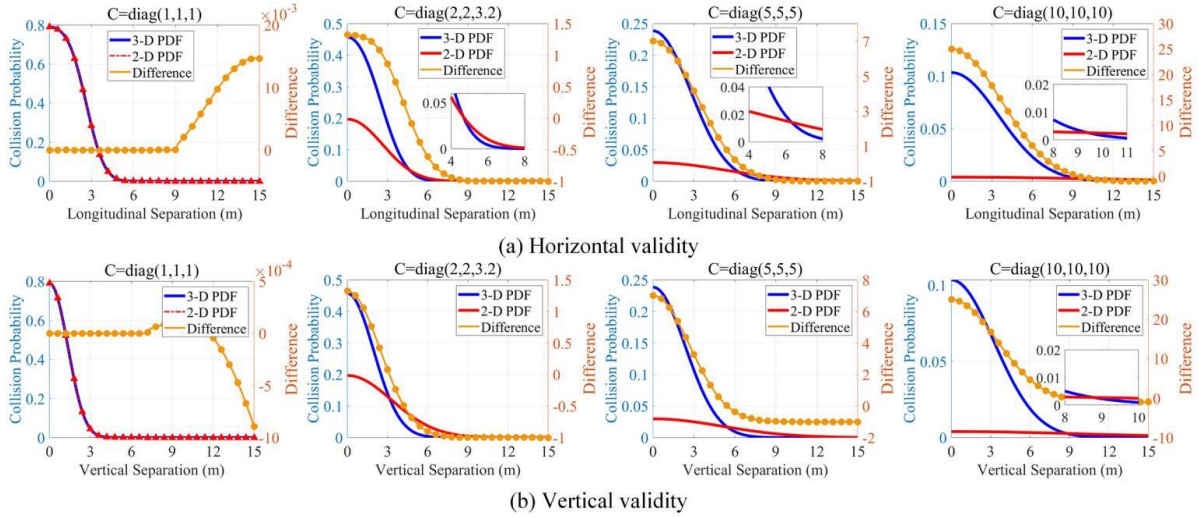

Fig. 22. Immunity of trajectory error variation. The difference is obtained by $(P_{3D} - P_{2D})/P_{2D}$.

图 22. 轨迹误差变化的免疫力。差异是通过 $(P_{3D} - P_{2D})/P_{2D}$ 获得的。

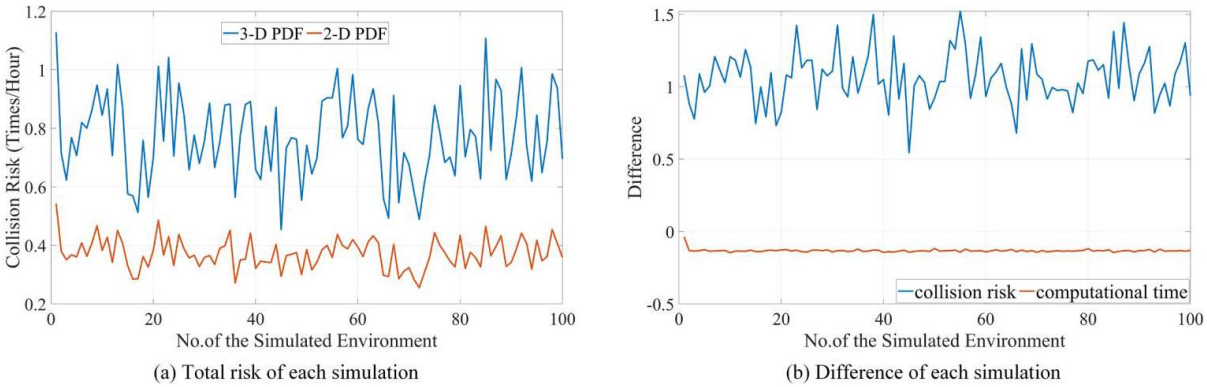

Fig. 23. Reliability analysis. The difference is obtained by $(CR_{3D} - CR_{2D})/CR_{2D}$ and $(T_{3D} - T_{2D})/T_{2D}$ respectively.

图 23. 可靠性分析。差异分别通过 $(CR_{3D} - CR_{2D})/CR_{2D}$ 和 $(T_{3D} - T_{2D})/T_{2D}$ 获得的。

5.4. Crossing routes

5.4. 交叉航线

Crossing routes refer to a certain angle α between the two routes whether the intersection exist, since the tracks could be set antar-afacially. In the section, to demarcate the minimum separations when fly over the intersection, we assume that there is a convergence point between two tracks, as shown in Fig. 18. Furthermore, align with the conservative principle, the extreme cases could provide references for selections between longitudinal and relative separation in Table 1. Compared to the scenarios above, the relative speed is divided into two directions, Along the Reference Direction (ARD) and Perpendicular to the Reference Direction (PRD). Therefore, the collision risk refers to the sum as

交路线指的是两条路线之间是否存在一定角度 α 的交叉，因为轨道可以设置为面对面。在本节中，为了划分在交叉点上空飞越时的最小间隔，我们假设两条轨道之间存在一个收敛点，如图 18 所示。此外，遵循保守原则，极端情况可以为表 1 中的纵向和相对间隔选择提供参考。与上述情况相比，相对速度分为两个方向，沿着参考方向 (ARD) 和垂直于参考方向 (PRD)。因此，碰撞风险指的是总和

$$F(t) = F_{ARD}(t) + F_{PRD}(t) \tag{27}$$

Let $\text{Sep}_{CPA} = 0$ m denotes the separation of the CPA is 0 . In this paper, the sUAVs converge at a speed of $6\ \text{m/s}$ with 30 m from the horizontal and vertical intersections. Noted that the results are no longer compared with the 5% sNMAC, due to the results above. Assume the angle ranges from 20° to 160° , with 5° each step. According to Fig. 19, the collision risk is in proportion to the volume, especially the crossing angle is 90°

令 $\text{Sep}_{CPA} = 0$ m 表示 CPA 的间隔为 0。在本文中，小型无人机 (sUAVs) 以 $6\ \text{m/s}$ 的速度从水平和垂直交叉点收敛，30 m 。需要注意的是，由于上述结果，结果不再与 5% sNMAC 进行比较。假设角度范围从 20° 到 160° ，5° 每一步。根据图 19，碰撞风险与体积成正比，尤其是当交叉角度为 90° 时

The collision risk also performs symmetrical distribution of angles with same separations, while the reaction tends to be imperceptible when the relative separation is greater than 6 m . The separations at the 'ELoS' are computed, which presents the minimum safety separations of different collision zones under different route angles as shown in Fig. 19. However, the results indicate that the separations should be selected reasonably when the relative movements change quickly, e.g., crossing angle is greater than 135° . Additionally, it is necessary to take diagonal distance of cuboid into account when the crossing angle is 90°

碰撞风险也表现出相同间隔角度的对称分布，而当相对间隔大于 6 m 时，反应趋向于不明显。计算了'ELoS' 的间隔，这表示在不同路线角度下不同碰撞区域的最小安全间隔，如图 19 所示。然而，结果表明，当相对运动快速变化时，例如，交叉角度大于 135° ，应合理选择间隔。此外，当交叉角度为 90° 时，有必要考虑立方体对角线的距离。

Similarly, the results of vertical convergence are depicted in Fig. 20. Predictably, the collision risk is in correlation with the relative distance and shape volume, while sphere has the most conservative performance in the determination. However, the overall risk has increased significantly, especially the angle is less than 90° , which caused the asymmetric change of collision risk. During the flight process in vertical scenario, the time periods and the vertical asymmetry of collision zones are different even with the same separation. The result indicates that we ought to be cautious when the sUAVs conduct the level changes with at acute angle. Consequently, the separation demarcated in different encountering scenarios is summarized in Fig. 21.

同样，图 20 描述了垂直收敛的结果。如预期，碰撞风险与相对距离和形状体积相关，而球体在确定中表现最为保守。然而，整体风险显著增加，特别是当角度小于 90° 时，这导致了碰撞风险的不对称变化。在垂直场景的飞行过程中，即使分离距离相同，碰撞区域的时间跨度和垂直不对称性也有所不同。该结果表明，当 sUAVs 以锐角进行水平变换时，我们应当谨慎。因此，不同相遇场景下的分离界限在图 21 中进行了总结。

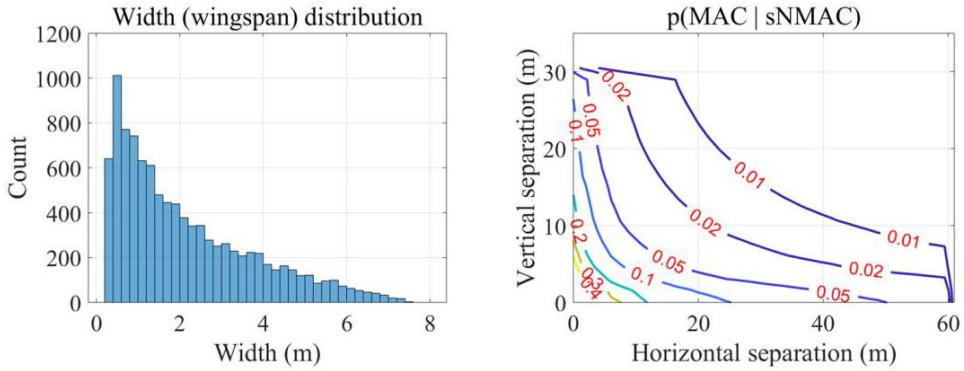

Fig. 24. Separations candidates by sNMAC-Initial software.
图 24。sNMAC-Initial 软件确定的分离候选方案。

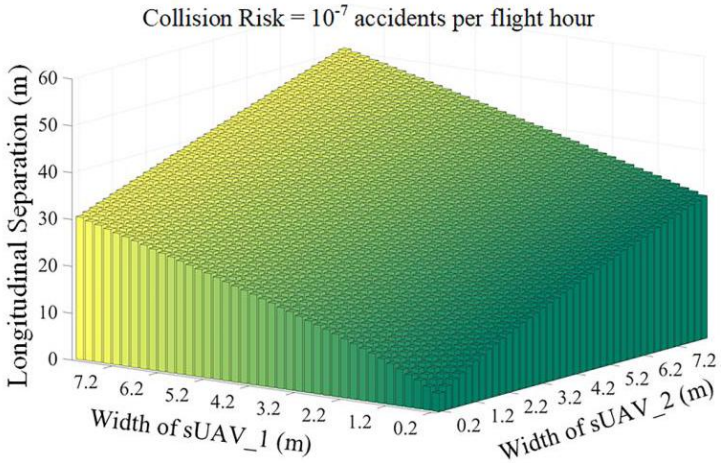

Fig. 25. Separations candidates by proposed model.
图 25。所提出模型确定的分离候选方案。

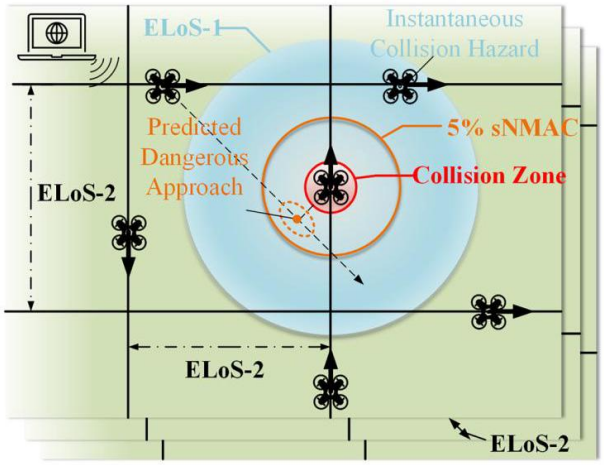

Fig. 26. The conceive of the separation criterion for sUAVs operating in the structured airspace.
图 26。在结构化空域中运行的 sUAVs 分离标准的构想。

5.5. Comparison analysis

5.5. 对比分析

Above, the separation demarcation method is established based on 3- D collision risk model. To demonstrate the advantages of the proposed model, the comparison analysis is conducted with 2-D collision risk model and sNMAC-Initial software. Here, the 2-D collision risk model refers to the risk calculated separately from the horizontal and vertical dimensions [30,49,63]. The sNMAC-Initial software is utilized and released by MIT LL in Ref. [13].

如上所述，分离界限方法是基于 3-D 碰撞风险模型建立的。为了证明所提模型的优点，我们与 2-D 碰撞风险模型和 sNMAC-Initial 软件进行了对比分析。此处，2-D 碰撞风险模型指的是分别从水平和垂直维度计算的风险 [30,49,63]。sNMAC-Initial 软件在文献 [13] 中由 MIT LL 使用并发布。

5.5.1. Reliability analysis of proposed model

5.5.1. 所提模型的可靠性分析

To test the reliability of proposed model in different environment with operational dynamics, e.g., navigation instability, random velocity variation. The collision risk model with 2-D PDF is utilized as a basis for comparison which was regarded as a efficient algorithem for collision risk estimation before $[30, 49, 59, 63]$. Futhermore, the MATLAB Interal2 function acts as the exact solution, and the collision zone is set as the cylinder.

为了测试所提模型在不同操作动态环境中的可靠性，例如导航不稳定、随机速度变化，我们使用了带有 2-D PDF 的碰撞风险模型作为比较的基础，该模型之前被认为是碰撞风险评估的有效算法 $[30, 49, 59, 63]$ 。此外，MATLAB Interal2 函数作为精确解，碰撞区域被设置为圆柱体。

Firstly, we conduct the simulations with the same sUAVs encouters above and the discrete covariance $\mathbf{C}$ chosen between 1 and 10 m . The immunity of trajectory error variation is depicted in Fig. 22. Overall, compared with 2-D model, 3-D model performs well with more robust results to error variation. The gap tends to be proportional to the error in both horizontal and vertical dimensions. Meanwhile, aligned with the shape size, the 3-D one has a better capacity to capture the separation variation in critical scale, i.e.,3to 12 m . As the position maintenance is hard to be ensured in embryonic stage of UTM [56], the 3-D collision model could be considered as a more suitable and reliable solution for sUAVs.

首先，我们使用与上述相同的 sUAV 遭遇情况和在 1 到 10 m 之间选择的离散协方差 $\mathbf{C}$ 进行模拟。轨迹误差变化的免疫性在图 22 中有所描述。总体而言，与 2-D 模型相比，3-D 模型在误差变化方面表现出色，结果更加稳健。差距在水平和垂直维度上都与误差成比例。同时，与形状大小一致，3-D 模型在捕捉关键尺度 (即 3 到 12 m) 的分离变化方面具有更好的能力。由于在 UTM 的早期阶段很难保证位置维护 [56]，3-D 碰撞模型可以被视为 sUAVs 的更合适和可靠的解决方案。

Subsequently, 100 simulation environments are established with parameters set randomly, shown in Table 3. Each environment has 200 sUAVs, and the total risk is calculated by Eq. (25). Note that the approximate solution is not utilized to accelerate the computational process, and the trajectory error is set as the same as the size of sUAV. The results are presented in Fig. 23.

接着，建立了 100 个参数设置随机的模拟环境，如表 3 所示。每个环境有 200 个 sUAV，总风险通过公式 (25) 计算得出。注意，没有使用近似解来加速计算过程，轨迹误差被设置为与 sUAV 的大小相同。结果在图 23 中展示。

The average difference of collision risk is 106.41% , as the reduction of computational time is 13.23% . The results demonstrate that the proposed model is more sensitive to estimate condition changes, providing a greater safety margin. In summary, the 3-D collision risk model performs well in both solution quality and computational efficiency. The results also confirm that the separations demarcated by it could achieve more the practicality and reliability in dynamic environments.

碰撞风险的平均差异为 106.41% ，计算时间的减少为 13.23% 。结果表明，所提出的模型对估计条件变化更为敏感，提供了更大的安全边际。总之，3-D 碰撞风险模型在解决方案质量和计算效率方面都表现出色。结果还确认了它所划分的分离距离在动态环境中具有更高的实用性和可靠性。

5.5.2. Elaboration of separation criteria

5.5.2. 分离标准的阐述

Illustrated in Section 2.1, the sNMAC-Initial software was developed by MIT LL and John Hopkins University Applied Physics Laboratory (JHU APL) [64]. After setting the distribution of wingspan, height, and encountering assumptions, the unmitigated risk and the candidates are given by contour lines. Shown in Fig. 24, the left-skew distribution of wingspan is chosen which corresponds to current drone market. The detailed information could be found in Ref. [13,19].

如第 2.1 节所示，sNMAC-Initial 软件由麻省理工学院林肯实验室和约翰霍普金斯大学应用物理实验室 (JHU APL)[64] 开发。在设定翼展、高度和遭遇假设的分布后，给出了无缓解风险和候选者，由等高线表示。如图 24 所示，选择了左偏的翼展分布，这与当前无人机市场相符。详细信息可在参考文献 [13,19] 中找到。

Because the likelihood of MAC highly depends on the wingspan size, sensitivity to it could be essential to facilitate a meticulous separation framework. Instead of facing all sUAVs with wingspan less than 25ft (7.6m), the proposed model presents superior performance of size-based separation criteria by the same model settings, depicted in Fig. 25.

因为 MAC 的可能性高度依赖于翼展大小，对其敏感可能是促进精确分离框架的关键。而不是面对所有翼展小于 25ft (7.6m) 的 sUAVs，所提出的模型在相同的模型设置下，通过基于大小的分离标准表现出更优的性能，如图 25 所示。

6. Discussion

6. 讨论

To explicit the mechanism of separation criteria in intelligent UTM, the paper conducts a comprehensive analysis of demarcation process, containing shape size, navigation performance, and encountering scenarios, et.al. As revealed in Concept of Operations v2.0 [11], safe operations pertain to the safety of the transportation system by multi-layers of separation assurance. By adopting the safety target of 'ELoS' and 5 % sNMAC, the method shows the efficiency and reliability to establish the holistic framework of separations for sUAVs (see Fig. 26). Therefore, commensurate with different functions, the framework is proposed to underpin the safety by four kinds of separations collectively, summerized in Table 4.

为了明确智能 UTM 中分离标准的机制，本文对划分过程进行了全面分析，包括形状大小、导航性能和遭遇场景等。如操作概念 v2.0[11] 所示，安全操作涉及通过多层分离保证来保障运输系统的安全。通过采用“ELoS”安全目标和 5%sNMAC，该方法展示了建立 sUAVs 整体分离框架的效率和可靠性 (见图 26)。因此，根据不同的功能，该框架被提议通过四种分离方式共同支撑安全，总结在表 4 中。

- Collision Zone. It is shaped by the actual size of sUAVs with a geometric extension. Intrusion of it is considered as a collision, which is intolerable.
- 碰撞区。它由 sUAVs 的实际大小和几何扩展形成。对其的入侵被视为碰撞，这是不可接受的。
- Collision Boundary. The volume is demarcated by the 5% sNMAC, which is utilized for incidents report and collision avoidance. The radius of it is determined by contour line at 5% collision probability.
- 碰撞边界。该体积由 5% sNMAC 划定，用于事故报告和避碰。其半径由 5% 碰撞概率的等高线确定。
- Self-Separation Volume. The region of 'ELoS-1' corresponding to the results in the paper serves as the well-clear volume to maintain safety criteria between each other. It is utilized to the sense of potential approach or hazards. Subsequently, it will help to achieve the target safety level of airspace, if each well clear is assured.
- 自分离体积。论文中对应的'ELoS-1' 区域作为保持彼此安全准则的清晰体积。它用于感知潜在的接近或危险。随后，如果每个清晰体积得到保证，它将有助于实现空域的目标安全水平。
- Structure of Air Route. 'ELoS-2' is the safety level oriented to operational airspace. The lateral separations specify the width of centrelines in tube-type routes. The vertical separations are achieved by requiring sUAVs using height-setting procedures to operate at different levels expressed in terms of flight levels or altitudes. Both can be considered as the separations of the structured air routes which will resolve the conflicts mostly from the strategic aspect.

- 空中航线结构。'ELoS-2' 是面向运营空域的安全水平。横向间隔规定了管型路线中中心线的宽度。垂直间隔是通过要求 sUAV 使用高度设置程序在不同飞行级别或高度上运行来实现的。这两者都可以被视为结构化空域的间隔，这将主要从战略角度解决冲突。

Once the airspace structure is established before flights, the well-clear or collision boundary will be assured by flight schedule, where the distance-based separations could be transformed into time slots for passing the intersection, e.g., the 4-D path planning. Also, the threshold could be down-selected to achieve more safety boundaries.

一旦在飞行前建立空域结构，清晰或碰撞边界将由飞行计划保证，其中基于距离的间隔可以转换为通过交叉点的时间槽，例如，4-D 路径规划。此外，可以将阈值降低以实现更多的安全边界。

Currently, the management tools are considered as a trade-off between the flight constraints (airspace structure) and efficiency. Since there are no recommended separation candidates for sUAV-only encounters in structured airspace. the original separation volume may significantly increase the alert rate of ACAS sXu in determined operations. Meanwhile, the global threshold as 'ELoS' is more explicit for regulatory departments, rather than local metric as sNMAC.

目前，管理工具被视为飞行约束 (空域结构) 和效率之间的权衡。由于在结构化空域中没有针对仅 sUAV 相遇的推荐间隔候选方案，原始间隔体积可能会显著增加 ACAS sXu 在确定操作中的警报率。同时，作为'ELoS' 的全局阈值对于监管机构来说更为明确，而不是作为局部指标的 sNMAC。

The ACAS for rotary UAVs in Urban Air Mobility (UAM) applications is being designed in coordination with RTCA, i.e., SC-147 [13], the 'ELoS' could be added in separation candidates in an iterative process, and recommended in final review. Meanwhile, when developing performance requirements for DAA in UAM, the aviation safety community should take the overall consideration of other management tools to avoid resource waste, such as flight procedure and airspace structure. The efforts in the paper also presume that the separation criteria are different from shape size, and performance. That is, however without validation, an elaborative separation framework.

用于城市空中出行 (UAM) 应用的旋翼无人机 ACAS 正在与 RTCA 协调设计，即 SC-147 [13]，'ELoS' 可以在迭代过程中添加到分离候选中，并在最终审查中推荐。同时，当为 UAM 中的 DAA 开发性能要求时，航空安全界应综合考虑其他管理工具，以避免资源浪费，例如飞行程序和空域结构。论文中的努力也假设分离标准因形状大小和性能的不同而不同，然而，未经验证，这是一个详尽的分离框架。

For regulatory bodies such as the FAA and EASA, the incorporation of quantitative performance requirements facilitates a clearer delineation of responsibility for separation provision in tandem with operational authorization. The cybersecurity architectures and level classifications become more discernible when juxtaposed with a recommended collision risk model and an encompassing safety target. Following this, the cooperative traffic management system will be tailored to accommodate a diverse range of operations, extending beyond just Class G airspace [3]. Additionally, the efficacy of operations will be enhanced through both in-flight and pre-flight guidance pertaining to separations.

对于 FAA 和 EASA 等监管机构来说，纳入定量性能要求有助于更清晰地划分与运营授权相伴的分离规定的责任。当与推荐的碰撞风险模型和全面的安全目标并置时，网络安全架构和级别分类变得更加明显。在此基础上，合作交通管理系统将被调整，以适应各种不同的运营，而不仅仅是 G 类空域 [3]。此外，通过飞行前和飞行中的分离指导，将提高运营的有效性。

The integration of risk-based separation paradigms can potentially augment the design and operational mitigation mechanisms pivotal for risk assessment guidelines, as exemplified by ICAO 9854 and SORA. For illustration, the granular design of airspace, coupled with the probabilistic models tailored for sUAVs, can bolster the feedback mechanisms essential for risk mitigation, as components currently absent in guidance documents like SORA Annex C [35]. Concurrently, by distinctly categorizing various separation layers, one can integrate time-constrained procedures, encompassing considerations such as exposure duration to potential risks. For entities like JARUS, which serve as guidance organizations, methodologies informed by the TPR could be extrapolated to conceive a more holistic framework for risk class determination. Additionally, it's noteworthy that separations might exhibit variations contingent on ground-level buffers and population densities.

风险基础分离范式的整合有可能增强风险评估指南设计及运营缓解机制的重要性，正如国际民航组织 (ICAO)9854 和 SORA 所例证的那样。例如，空域的细化设计与针对小型无人机 (sUAVs) 的概率模型相结合，可以加强对于风险缓解至关重要的反馈机制，这是像 SORA 附录 C [35] 这样的指导文件目前所缺乏的组成部分。同时，通过明确分类各种分离层，可以整合时间受限的程序，包括考虑到潜在风险的暴露时长。对于像 JARUS 这样的指导组织，可以根据总体性能指标 (TPR) 提出的方法，推断出用于风险等级确定的更全面框架。此外，值得注意的是，分离距离可能会根据地面缓冲区和人口密度表现出变化。

Table 4
表 4
Multi-layer separations for sUAVs.
针对小型无人机的多层分离。

Separations	Number of sUAVs	Threshold	Utilization
Collision Zone	1	Size of sUAV	Collision Determination
Collision Boundary	2	Collision probability= 0.05	Collision Avoidance
ELoS-1	2	Collision Rate=1.5*10*	Well Clear Volume
ELoS-2	N	Collision Rate=10	Air Route Design

分离距离	小型无人机的数量	阈值	利用率
碰撞区域	1	小型无人机的尺寸	碰撞判定
碰撞边界	2	碰撞概率 = 0.05	避碰
ELoS-1	2	碰撞率 = 1.5*10*	清晰空间体积
ELoS-2	N	碰撞率 = 10	航路设计

7. Conclusions

7. 结论

Separation for UTM is an essential enabler for the safe conduct of operations, from strategic flight planning, management tools to tactical UAVs avoidance capabilities. For the problem that few researches of separation criteria focus on sUAVs-only encounters and low-altitude airspace design [13], which also take few considerations on the concept of multi-layer separations. In this paper, the separation demarcation method has been studied based on collision risk model and safety threshold. The main conclusions are summarized.

对于无人交通管理系统 (UTM) 来说，分离是确保安全运行的关键使能因素，从战略飞行计划、管理工具到战术无人机避障能力。目前关于分离标准的研究很少关注仅限于小型无人机的遭遇以及低空空域设计 [13]，也很少考虑到多层分离的概念。在本文中，基于碰撞风险模型和安全阈值研究了分离界限方法。主要结论如下。

1 The method is effective and reliable to demarcate the self-separations for sUAVs in structured low-altitude airspace. The experiments of different scenarios shows that the adoption of 'ELoS' provides the fundamental guarantee to maintain well clear for drone-only encounters, which is compatible with 5% sNMAC. Moreover, the method may help to formulate the elaborative, multi-dimensional separation criteria for UTM to design and evaluate airspace and collision avoidance.

1 该方法在结构化低空空域中为小型无人机划设自我分离区域是有效且可靠的。不同场景的实验表明，采用“ELoS”为仅限于无人机遭遇提供了保持清晰间隔的基本保障，这与 5% sNMAC 兼容。此外，该方法可能有助于为 UTM 制定和评估空域和避障的详尽、多维分离标准。

2 The collision risk model proposed in the paper could capture the peculiarities of shape size, maneuverability, navigation performance, and encountering scenarios. The 3-D collision risk model achieves more safety margin and efficiency on critical scale than the traditional method. Also, the supremum of trajectory deviation is determined by sensitivity analysis to meet the requirements of conservative risk assessment and real-time calculation, with 106.41% in average difference and 13.23% in reduction of computational time.

本文提出的碰撞风险模型能够捕捉形状大小、操控性、导航性能和遭遇场景的特殊性。三维碰撞风险模型在关键尺度上比传统方法具有更大的安全边际和效率。此外，通过敏感性分析确定轨迹偏差的最大值，以满足保守风险评估和实时计算的要求，平均差异为 106.41% ，计算时间减少为 13.23% 。

3 The paper redefined the sNMAC volume based on the geometrical extension, which is called the collision zone. To provide an overall analysis of shape characteristics, we summarized the existing shapes with a minimum envelope shape. The results show that the volume serves the significant role in risk estimation, especially where the collision is about to occur. Combined with computational time, ellipsoid and cylinder are recommended to achieve a better balance between safety margin and operational efficiency. And it is helpful to design the crossing route with angles around 90° Additionally, the combined zone provides the baseline to conduct risk estimation for UTM in the future.

本文基于几何扩展重新定义了 sNMAC 体积，称之为碰撞区。为了提供形状特性的全面分析，我们总结了现有的最小包络形状。结果显示，该体积在风险评估中起着重要作用，特别是在即将发生碰撞的情况下。结合计算时间，推荐使用椭球体和圆柱体以实现安全边际和操作效率之间的更好平衡。并且，在角度约为 90° 的情况下设计交叉路线是有帮助的。此外，结合区域为未来进行 UTM 风险评估提供了基准。

Nevertheless, the baselines of distanced-based separations do not provide maneuvering spaces which result in the absence of safety bound for retardation [42]. Also, since there is no clear classification of sNMAC based on characteristics of sUAV, e.g., fixed wing or rotary wing, long-range or low cost, size, weight, and power (low-C-SWaP) [13]. In the future, retrofitting of sNMAC should be accomplished by realistic operations in structured airspace, and separation demarcation should take the capacity of individuality into account to form a dynamic

criterion. For instance, if the ADS-B is equipped on all the sUAVs (like traditional aviation), it will be more intelligent for sUAVs to sense and avoid the collision with data sharing. Additionally, more flight trials are required to capture dynamic factors such as human interference and turbulences in low-altitude airspace. In other words, the conception of separations in UTM is being reimaged, much more effects are still required to make these methods robust and implementable for real-world sUAV operations.

然而，基于距离的分离基线并未提供足够的机动空间，这导致减速 [42] 的安全边界缺失。此外，由于没有根据 sUAV 的特性 (例如固定翼或旋翼、远程或低成本、尺寸、重量和功率 (低 C-SWaP)[13]) 对 sNMAC 进行明确的分类。未来，sNMAC 的改造应通过结构化空域中的实际操作来完成，分离划界应考虑个体容量，形成动态标准。例如，如果所有 sUAV 都装备了 ADS-B(如同传统航空)，通过数据共享，sUAV 感知和避免碰撞将更加智能。此外，还需要进行更多的飞行试验来捕捉低空空域中的动态因素，如人为干扰和湍流。换句话说，UTM 中的分离概念正在被重塑，仍需更多的工作来使这些方法在现实世界的 sUAV 运作中变得健壮和可行。

CRediT authorship contribution statement

贡献声明

Gang Zhong: Validation, Methodology, Funding acquisition, Conceptualization. Sen Du: Software, Methodology, Conceptualization, Visualization, Writing - original draft. Honghai Zhang: Supervision, Project administration, Investigation, Funding acquisition. Jiangying Zhou: Visualization, Validation, Resources, Formal analysis, Data curation. Hao Liu: Validation, Supervision, Investigation.

洪中: 验证、方法论、资金获取、概念构思。杜森: 软件、方法论、概念构思、可视化、撰写 - 原始草稿。张洪海: 监督、项目管理、调查、资金获取。周姜英: 可视化、验证、资源、形式分析、数据整理。刘浩: 验证、监督、调查。

Declaration of Competing Interest

利益冲突声明

The authors declare that they have no known competing financial interests or personal relationships that could have appeared to influence the work reported in this paper.

作者声明，他们没有已知的经济利益或个人关系可能影响本文报告的工作。

Data availability

数据可用性

No data was used for the research described in the article.

文章描述的研究未使用任何数据。

Acknowledgement

致谢

The work described in this paper was substantially supported by the Fundamental Research Funds for the Central Universities, NO. NS2023037, Postgraduate Research & Practice Innovation Program of NUAA, NO. xcxjh20230745, and National Natural Science Foundation of China, NO. 71971114 and U2133207. The authors also wish to express their gratitude to the anonymous reviewers for their valuable suggestions and comments, which have significantly improved the quality of this article.

本文的研究工作得到了中央高校基本科研基金的支持，项目编号为 NS2023037，南京航空航天大学研究生科研与实践创新项目编号为 xcxjh20230745，以及国家自然科学基金的支持，项目编号为 71971114 和 U2133207。作者们也愿向匿名审稿人表示感谢，他们的宝贵建议和评论显著提高了本文的质量。

References

参考文献

[1] Garrow LA, German BJ, Leonard CE. Urban air mobility: a comprehensive review and comparative analysis with autonomous and electric ground transportation for https://doi.org/10.1016/j.trc.2021.103377.

[2] Cohen AP, Shaheen SA, Farrar EM. Urban air mobility: history, ecosystem, market potential, and challenges. IEEE Trans Intell Transp Syst 2021;22:6074-87. https:// doi.org/10.1109/TITS.2021.3082767.

[3] Bauranov A, Rakas J. Designing airspace for urban air mobility: a review of concepts and approaches. Prog Aerosp Sci 2021;125. https://doi.org/10.1016/j.paerosci.2021.100726.[4] Pang B, Hu X, Dai W, Low KH. UAV path optimization with an integrated cost assessment model considering third-party risks in metropolitan environments. Reliab Eng Syst Saf 2022;222. https://doi.org/10.1016/j.ress.2022.108399.

[5] Blom HAP, Jiang C, Grimme WBA, Mitici M, Cheung YS. Third party risk modelling of unmanned aircraft system operations, with application to parcel delivery service. Reliab Eng Syst Saf 2021;214. https://doi.org/10.1016/j.ress.2021.1077

[6] Liu T, Bai G, Tao J, Zhang YA, Fang Y. A multistate network approach for resilience Engineering & System Safety; 2023. https://doi.org/10.1016/j.ress.2023.109606.

[7] Liu L, Yang J. A dynamic mission abort policy for the swarm executing missions and its solution method by tailored deep reinforcement learning. Reliab Eng Syst Saf 2023;234. https://doi.org/10.1016/j.ress.2023.109149.environments by conflict resolution. Transp Res Part C: Emerg Technol 2021;131. https://doi.org/10.1016/j.trc.2021.103355.

[9] Bertram J, Wei P, Zambreno J. A fast markov decision process-based algorithm for collision avoidance in urban air mobility. IEEE Trans Intell Transp Syst 2022;23: 15420-33. https://doi.org/10.1109/tits.2022.3140724.

[10] Yang X, Wei P. Autonomous free flight operations in urban air mobility with computational guidance and collision avoidance. IEEE Trans Intell Transp Syst 2021;22:5962-75. https://doi.org/10.1109/tits.2020.3048360.2022.https://www.faa 08/UTM_ConOps_v2.pdf.

[12] ICAO. Unmanned Aircraft Systems (UAS). International civil aviation organization. 2023. https://www.icao.int/NACC/Docu NACCWG8-P02-Eng.pdf.

[13] Weinert A, Alvarez L, Owen M, Zintak B. Near midair collision analog for drones based on unmitigated collision risk. J Air Transportation 2022;30:37-48. https:// doi.org/10.2514/1.D0260. 10.1016/j.ress.2022.108410.

[15] FAA. Order Jo 7110.65AA - Air Traffic control. Federal Aviation Administration; 2023. https://www.faa.gov/documentLibra c_dtd_4-20-23_FINAL.pdf.

[16] Zhang Y, Shortle J, Sherry L. Methodology for collision risk assessment of an airspace flow corridor concept. Reliab Eng Syst Saf 2015;142:444-55. https://doi.org/10.1016/j.ress.2015.05.015.separation for urban air mobility operations in uncertain environments. IEEE Trans Intell Transp Syst 2022;23:19413-27. https://doi.org/10.1109/tits.2022.31636

[18] Lester ET, Weinert A. Three quantitative means to remain well clear for small UAS in the terminal area. 2019 integrated communications. Navigation and Surveillance Conference (ICNS); 2019. p. 1-17. https://doi.org/10.1109/ ICNSURV.2019.8735171.

[19] Weinert AJ, Campbell SE, Vela AE, Schuldt DW, Kurucar JA. Well-clear

[20] Deaton J., Owen M.P. Evaluating collision avoidance for small UAS using ACAS X. AIAA Scitech 2020 Forum. 2020. 10.2514/6.2020-0488.

[21] RCTA. SC-147, traffic alert & collision avoidance system (TCAS). Radio Technical Commission for Aeronautics; 2023. https://www.rtca.org/sc-147/.

[22] Alvarez LE, Jessen I, Owen MP, Silbermann J, Wood P. ACAS sXu: robust decentralized detect and avoid for small unmanned aircraft systems. In: 2019 IEEE/AIAA 38th Digital Avionics Systems Conference (DASC); 2019. p. 1-9.

[23] Shao Q, Li R, Dong M, Song C. An adaptive airspace model for quadcopters in urban air mobility. IEEE Trans Intell Transp Syst 2022:1-10. https://doi.org/ 10.1109/tits.2022.3219815.

[24] Kim J, Atkins E. Airspace geofencing and flight planning for low-altitude, urban, small unmanned aircraft systems. Appl Sci 2022;12. https://doi.org/10.3390/ app12020576.

[25] National Academies of Sciences E. Medicine. assessing the risks of integrating unmanned aircraft systems (UAS) into the national airspace system. Washington,

[26] Clothier RA, Williams BP, Fulton NL. Structuring the safety case for unmanned aircraft system operations in non-segregated airspace. Saf Sci 2015;79:213-28. https://doi.org/10.1016/j.ssci.2015.06.007.

[27] ICAO. Doc 7300 Convention on International Civil aviation. International Civil Aviation Organization Montréal; 2006.

[28] ICAO. Doc 9689 manual on airspace planning methodology for the determination of separation minima. International Civil Aviation Organization Montréal; 1998. [29] Young R. Advances in UAS ground-based detect and avoid capability. 2019 p. 1-14. https://doi.org/10.1109/ICNSURV.2019.8735385.

[30] Lu F, Chen Z, Chen H. Lateral collision risk assessment of parallel routes in ocean area based on space-based ads-b, 124. Transportation Research Part C: Emerging Technologies; 2021. https://doi.org/10.1016/j.trc.2021.102970.

[31] Pang B, Ng EM, Low KH. UAV trajectory estimation and deviation analysis for contingency management in urban environments. AIAA AVIATION 2020 FORUM; 2020. https://doi.org/10.2514/6.2020-2919.[32] Pang B, Zhang M, Deng C, Low KH. Investigation of flight technical error for UAV separation requirement based on flight trajectory data. AIAA AVIATION 2022 FORUM; 2022. https://doi.org/10.2514/6.2022-3763.

[33] Zou Y, Zhang H, Zhong G, Liu H, Feng D. Collision probability estimation for small unmanned aircraft systems. Reliab Eng Syst Saf 2021;213(3):107619. https://doi.org/10.1016/j.ress.2021.107619.

[34] RCTA. SC-228, minimum operational performance standards (MOPS) for detect and avoid (DAA) systems. 2022. https://www.rtca.org/sc-228/.Rulemaking of Unmanned Systems; 2023. http://jarus-rpas.org/wp-content/uploa ds/2023/07/jar_doc_06_jarus_sora_v2.0.pdf.

[36] Pang B, Low KH, Lv C. Adaptive conflict resolution for multi-UAV 4D routes optimization using stochastic fractal search algorithm. Transp Res Part C: Emerg

Technol 2022;139:103666. https://doi.org/10.1016/j.trc.2022.103666.doi.org/10.1109/TITS.2018.2839344.

Technol 2022;139:103666. https://doi.org/10.1016/j.trc.2022.103666.doi.org/10.1109/TITS.2018.2839344.

[37] Weibel R, Edwards M, Fernandes C. Establishing a risk-based separation standard for unmanned aircraft self separation. Ninth USA/Europe Air Traffic Management Research & Development Seminar; 2011. p. 14-7. https://doi.org/10.2514/

[38] Chen C, Edwards MWM, Gill B, Smearcheck S, Adami T, Calhoun SM, et al. Defining well clear separation for unmanned aircraft systems operating with noncooperative aircraft. AIAA Aviation 2019 Forum; 2019. https://doi.org/ 10.2514/6.2019-3512.

[39] Munoz C, Narkawicz A, Chamberlain J, Consiglio MC, Upchurch JM. A family of well-clear boundary models for the integration of UAS in the NAS. In: 14th AIAA aviation technology, Integration, and operations conference; 2014. https://doi.org/10.2514/6.2014-2412.requirements.2023.10.1520/F3442_F3442M-20.

[41] Wu MG, Cone AC, Lee S, Chen C, Edwards MW, Jack DP. Well clear trade study for unmanned aircraft system detect and avoid with non-cooperative aircraft. In: 2018 Aviation technology, integration, and operations conference; 2018. https://doi.org/10.2514/6.2018-2876.

[42] Hu J, Erzberger H, Goebel K, Liu Y. Probabilistic risk-based operational safety bound for rotary-wing unmanned aircraft systems traffic management. J Aerospace in urban environments. IEEE Trans Veh Technol 2021;70:7464-79. https://doi.org/10.1109/tvt.2021.3093318.

[44] Tang J, Liu G, Pan Q. A review on representative swarm intelligence algorithms for solving optimization problems: applications and trends. IEEE/CAA J Autom Sin 2021;8:1627-43. https://doi.org/10.1109/JAS.2021.1004129.

[45] Dai W, Pang B, Low KH. Conflict-free four-dimensional path planning for urban air mobility considering airspace occupancy. Aerosp Sci Technol 2021;119. https://

[46] Delamer JA, Watanabe Y, Chanel CPC. Solving path planning problems in urban environments based on a priori sensors availabilities and execution error propagation. AIAA Scitech 2019 Forum; 2019. https://arc.aiaa.org/doi/abs/10.2514/6.2202.

[47] Reich PG. Analysis of long-range air traffic systems: separation standards-I. J Navig 1966;19:88-98. https://doi.org/10.1017/s0373463300019068.

[48] Siddiqee W. A mathematical model for predicting the number of potential conflict situations at intersecting air routes. Transp Sci 1973;8:58-64. https://doi.org/

[49] Mitici M, Blom HAP. Mathematical models for air traffic conflict and collision probability estimation. IEEE Trans Intell Transp Syst 2019;20:1052-68. https://

[50] Brooker PI. Longitudinal collision risk for ATC track systems: a hazardous event model. J Navig 2005;59:55-70. https://doi.org/10.1017/S0373463305003516.

[51] Brooker PI. Lateral collision risk in air traffic track systems: a 'post-reich' event

[52] Paielli RA, Erzberger H. Conflict probability estimation generalized to non-level flight. Air Traffic Control Q 1999;7(3):195-222. https://doi.org/10.2514/ atcq.7.3.195.

[53] Zhang N, Liu H, Low KH. UAV collision risk assessment in terminal restricted area by heatmap representation. AIAA SCITECH 2023 Forum; 2023. https://arc.aiaa.or g/doi/abs/10.2514/6.2023-0737.

[54] Paielli RA, Erzberger H. Conflict probability estimation for free flight. J Guidance Control Dyn 1997;20(3):588-96. https://doi.org/10.2514/6.1997-1.international civil aviation organization implementation. Trans Aerospace Res 2019:53-64. https://doi.org/10.2478/tar-2019-0005.

[56] Wang CHJ, Ng EM, Low KH. Investigation and modeling of flight technical error (FTE) associated with UAS operating with and without pilot guidance. IEEE Trans Veh Technol 2021;70:12389-401. https://doi.org/10.1109/tvt.2021.31170

[57] Zhang G, Hsu LT. Intelligent GNSS/INS integrated navigation system for a commercial UAV flight control system. Aerosp Sci Technol 2018;80:368-80.

[58] Kallinen V, Martin T, Mcfadyen A. Required navigation performance specifications for unmanned aircraft based on UTM flight trials. In: 2020 international conference on unmanned aircraft systems; 2020. p. 196-203. https://doi.org/10.1109/ ICUAS48674.2020.9213980.

[59] McFadyen A. Probabilistic determination of maximum safe altitudes for unmanned traffic management. In: 2019 IEEE/AIAA 38th digital avionics systems conference (DASC); 2019. p. 1-10. https://doi.org/10.1109/DASC43569.2019.90817

[60] Liu H, Zhu DW, Xie X, Chen J, Liu X. Optimization of lateral collision risk of aircraft 10.1155/2022/2002423.

[61] Xiong L. Research on collision risk of vertical separation minima based on EVENT model. J Civil Aviat Univ China 2008. https://doi.org/10.3969/j.issn.1001- 5590.2008.04.001.

[62] Kim SH. Conflict risk analysis of small unmanned aircraft systems. J Aerospace Inf Syst 2018;15:684–95. https://doi.org/10.2514/1.1010665.

[63] Yang L, Li W, Wang S, Zhao Z. Multi-attributes decision-making for CDO trajectory planning in a novel terminal airspace. Sustainability 2021;13. https://doi.org/

[64] Weinert A., Alvarez, L., Owen, M., and Zintak, B. ”sNMAC-Initial,”. March 2020. 10.5281/zenodo.3727764.